Master's Degree

In Conservation Science and Technologies for Cultural Heritage (LM-11)

Final Thesis

Dark Earth: characterization of post-classic urban stratification in Norther Italy

Supervisor
Prof. Dario Battistel

Assistant supervisor
Dr. Elena Argiriadis
Dr. Mara Bortolini

Graduand
Sofia Borghero
Matriculation number 847962

Academic Year
2018 / 2019

SUMMARY

1 SCOPE 4

2 INTRODUCTION 5

2.1 DARK EARTH: URBAN ARCHAEOLOGY CONTEXT 5

2.2 DARK EARTH: CHARACTERISTICS, HISTORY AND ORIGIN 6

3 HISTORICAL CONTEXT 10

3.1 RELATIONSHIP BETWEEN GERMANIC MIGRATION AND CLIMATE VARIATIONS 12

4 CHEMICAL MARKERS 14

4.1 DETECTION OF FIRE EVENTS 15

4.1.1 Charcoal 15

4.1.2 Polycyclic Aromatic Hydrocarbons 15

4.1.3 Anhydrous monosaccharides 17

4.2 *N*-ALKANES 18

4.3 HUMAN PRESENCE 19

4.3.1 Miliacin 19

4.3.2 Fecal, plant and fungal sterols 20

5 MATERIALS AND METHODS 22

5.1 STANDARDS AND REAGENTS 22

5.2 SAMPLING SITE 23

5.2.1 Verona 23

5.2.2 Mel 24

5.3 INSTRUMENTAL EQUIPMENT AND PROCEDURE 25

5.3.1 Extraction and volume reduction 25

5.3.2 Chromatographic analysis 26

5.4 ELEMENTAL ANALYZER 31

5.4.1 Charcoal analysis 31

6 RESULTS 33

6.1 VERONA: VICOLO SAN PIETRO IN MONASTERO (SPM) 33

6.1.1 Total and organic carbon 33

6.1.2 Polycyclic Aromatics Hydrocarbons (PAHs) 34

6.1.3 n-Alkanes 36

6.1.4 Charcoal analysis 40

6.1.5 Anhydrous monosaccharides (AMs) 41

6.1.6 Miliacin 44

6.1.7 Fecal, plants and fungal sterols (FPFS) 46

6.2 VERONA: VIA PIGNA (VP) 48
6.2.1 Total and organic carbon 48
6.2.2 Polycyclic Aromatics Hydrocarbons (PAHs) 49
6.2.3 n-Alkanes 51
6.2.4 Charcoal analysis 54
6.2.5 Anhydrous monosaccharides (AMs) 55
6.2.6 Miliacin 58
6.2.7 Fecal, plants and fungal sterols (FPFS) 60
6.3 BELLUNO: MEL (MEL) 62
6.3.1 Total and organic carbon 62
6.3.2 Polycyclic Aromatics Hydrocarbons (PAHs) 62
6.3.3 n-Alkanes 63
6.3.4 Charcoal analysis 65
6.3.5 Anhydrous monosaccharides (AMs) 65
6.3.6 Miliacin 66
6.3.7 Fecal, plants and fungal sterols (FPFS) 67
7 DISCUSSION 68
7.1 VERONA: VICOLO SAN PIETRO IN MONASTERO (SPM) 69
7.2 VERONA: VIA PIGNA (VP) 70
7.3 BELLUNO: MEL (MEL) 71
7.4 COMPARISON BETWEEN THE SITES 72
8 CONCLUSIONS 77
9 REFERENCES 79

1 SCOPE

This thesis project is focused on the study of the Dark Earths (DE), urban stratifications dating back to the post-classic period. They have a dark color, according to the name, with a solid and homogeneous aspect. The DE are anthropic soils largely linked with human activities: for this reason, building fragments and remains can often be found. Many archaeologists are interested in this phenomenon; therefore, many studies are focused on their origin and many hypotheses have been formulated. The two main hypotheses related to the origin of the DE are (i) the waste origin and (ii) the agricultural soil origin.

The DE involved in this project are from Verona and from Mel (BL), both located in northern Italy. In particular, the Verona samples are from two archeological excavations: Vicolo San Pietro in Monastero (SPM) and Via Pigna (VP), while the Mel samples are from a single excavation.

The aim of this project is to characterize the organic fraction of DE in order to reconstruct their origin and everyday life activities of people living in the post-classic period. The investigations included in this work involve, in order to contribute to the identification of processes that originated DE, mainly chromatographic analyses of molecular proxies linked with charcoal distribution and analysis of total and organic carbon. With these analyses, it was possible to investigate chemical markers in order to reconstruct the origin of DE, in particular molecules that are related to detection of fire events and human contribution to transformations occurred in the archeological site.

2 INTRODUCTION

2.1 Dark Earth: urban archaeology context

The first findings of Dark Earth (DE) were accidentally, because they were found in the urban setting during road works and in construction sites. Not only DE were found in this way, but also other archaeological discoveries occur in this manner. For this reason, the archaeologists founded a new branch of archaeology: the urban archaeology. Until that moment, archaeological research focused on big construction projects such as the Roman *domus* or the Christian *basilicas*, giving less importance to the overall urban context. The first studies based on urban archaeology were developed in Winchester (London, UK) in the second half of the 1960s, then expanded to the rest of Europe [1]. In the '80s, the European cities development caused a large excavation requirement, pushing urban archaeology research to a very large expansion [1]. Urban archaeology represents a revolution in the strategy, in the methods and in the excavation procedures, and most of all in the treatment of historical findings [1]. Before developing urban archeology as a methodology, these findings were assigned to the builder or to the surveyor. Now these excavations are conducted under the supervision of archeologists that regulate the working procedures with specific methodology [2]. Urban archaeology highlighted the topography of post-classic cities, with their fortifications and the everyday life activities. These aspects were totally neglected before the 60's. Other aspects like productive activities, graveyards internal to the city walls and infrastructures, raised to attention from studies starting from the second half of the century, are now studied to better understand the ancient life.

Urban archaeology takes care of city transformation, above all the ones concerning the post-classic centuries (4^{th}- 7^{th} century), a very turbulent period on the historical, economic and social point of view. Looking at these stratifications, it is possible to see that the technologies employed were less sophisticated then the Roman ones [2]. Urban archaeology focuses also on this aspect, trying to detect the causes of this technological regression, where methods employed were more similar to prehistoric ones [2].

Archaeological stratigraphy is involved in giving a time framework to such findings. It takes inspiration from geology and its stratigraphic models, using a methodology that permits to outline the time sequence of the different layers in a profile [3]. The accumulations come from complex urban stratigraphic sequences. Urban sites are characterized by many phases of long-time human occupation resulting in the continuous accumulation of soil [4]. For this reason, the stratifications

found through urban archaeology are related to urban life aspects such as the infrastructures: drainage systems or the abandonment of waste on the streets and gardens are elements that caused accumulation of soil, often of several meters. It is very likely to find Dark Earths in such settings [2]. The deposition of these stratifications causes a radical change in the sedimentation rate and features, resulting in a clear discontinuity with previous layers [1].

2.2 Dark Earth: characteristics, history and origin

Dark Earth plays an important role in the vertical growth of the above-mentioned European urban stratifications. Dark Earth (DE) is a homogeneous (internal stratification is not evident), dark-colored horizontal layer often rich in anthropogenic remains [4]. These stratifications are strictly connected with urban archaeology, in fact they have been found exclusively in urban structures, far from rural contexts, so they are strongly related to human activities inside the cities [4].

The very first time that the name "*dark made earth"* appeared was in 1912. Norman and Reader used this definition to describe the level in between the stratifications from the Roman and medieval periods in the city of London [5]. The term "Dark Earth" was then used again in London during excavations performed in the 1970s and in the 1980s, when numerous DE were found above the Roman stratifications, in a context of urban archaeology [1]. Archaeologists dated the first DE found in Europe back to the period between the 5th and the 11th century, so it was possible to fill the previous historical gap, and gain knowledge about the post-classic period, in particular about the urban context [1]. Between the end of the '70s and the '80s, the urban excavations developed also in Italy, particularly in Milan where, during the 1982 subway works, numerous stratifications were found between the Roman and medieval layers, similarly to those found in other European cities including the English DE [6,7]. From the early '80s onwards, in other Italian cities, similar dark soil strata were found. In particular, in Mantua and in Cremona (Lombardia region) the *Notiziario Archeologico della Lombardia* reported DE findings during excavations [8]. Other dark soils were found in Bologna, during archeological survey at a Roman villa covered with a Dark Earth layer. In Brescia, again DE were found in a very thick layer [9]. In Verona, since 1981, many stratifications identified as DE were found in concomitance with different urban excavations in various parts of the city [10]. The DE discovery concerns also other cities: Trento, Florence, and Naples [11–13]. It was then evident that DE findings were not a limited phenomenon but a widespread occurrence that needed to be analyzed.

An important characteristic is related to the dark color of the Dark Earth: the color of soils mainly results from organic matter or humic substances. DE is also defined as “Humic horizon” [4], that is a layer of soil rich in humic constituents, the largest product of the organic biodegradation of perishable materials from plants and animals. In addition, human activities can cause the enrichment of organic matter in this soil, for example with fires or waste disposal [14]. Humic substances are the main responsible of complex chemical reactions in soils, indeed they can react with metal ions, oxides, hydroxides, minerals and other organic molecules forming water-soluble or water-insoluble compounds [15]. In DE, the dark color is not always related to a high organic content: some studies highlighted that the concentration of organic matter in DE samples is not as high as agricultural soils, and not enough to justify the black color [1]. About this purpose, Macphail (1983) promoted the hypothesis that the dark color was related to the combustion of organic materials: the charred material (in micrometric scale) distributed and dispersed in the matrix could have originated the black color, also because micro-carbon is often one of the major components detected in the DE [16]. One of the problems related to the micro-carbon particles is the differentiation between the micrometric material coming from burning events and the one resulting from the natural degradation of substances in the soil [1]. The main point of post-depositional fragmentation is the way in which the organic micro-particles become part of the layer and in what way the particles are fragmented. The possibilities are two: one is that the particles are already present, such as in the ashes from fireplaces disposed on the ground. The other one is related to bioturbation, that causes the mechanical fragmentation of originally bigger charcoal particles, these fragments are then dispersed in the matrix [17]. The charcoal found in the DE can give information about the soil destination, meaning that through the study of charred material it is possible to reconstruct the uses of soil. In particular, if charcoal originated by fire events is present (in the form of backfill material or added to the soil as fertilizer), an agricultural use is more probable. Conversely, if charcoal is found in association with other elements such as ash, bones and ceramic fragments, the soil had more likely a disposal destination [4]. Starting from charcoal fragments, it is also possible to identify plant species through the taxonomy: for example, Wiedner et al. 2015 identified fragments of burned logs of oak, alder, birch and hornbeam in the DE, from Germany, that he observed [18].

In order to reconstruct the overall composition of DE, the micromorphology approach can be useful to identify other fragments and inclusions such as bones, microfossils, phytoliths, minerals and anthropic artifacts, with their specific location [14]. Man-made materials such as bricks, shingles, ceramic, mosaic tesserae, stones, glass, or aggregates like mortars, plasters, remains of charcoal, of

metal manufacturing, can be found in DE stratifications [4,19]. Important information can be collected through particular marks found in the fragments of ceramic, remains of agricultural pits, charred seeds, and all the remains of humans activities [1]. In addition, the position of such remains in the stratification provides an interpretation of the deposition rate [20]. However, the complete absence of a predominant orientation and the mixing of materials associated to different ages, often found in the DE samples, defines a mainly homogeneous layer in which it becomes very difficult to define a temporality [5].

The components present in the DE give space to a lot of interpretations about their origin. In fact, the main problem is trying to identify the origin of these stratifications, because the term has become a general expression used in European urban archaeology to describe different layers with similar characteristics, not to identify a specific geological definition. Therefore, the term "Dark Earth" does not imply a univocal archaeological interpretation. For this reason, a perfect definition of DE is difficult to outline, since there is no description of what Dark Earth is or what it is not. Some hypotheses were promoted on the origin of DE. In particular, according to Macphail et al. (2013) and Macphail (1981) [5,21], there are two possible origins of DE: one related to urban cultivation and the other one linked to waste disposal. In fact, Macphail supposed that, after the Roman decline, people started to have vegetable gardens inside the city walls. Arthur (1991) [22], according to this supposition, pointed out that DE could be the result of backfilling for agricultural purposes. The hypothesis was supported by the ceramic fragments found in it, that revealed particular abrasion signs related to the use of a hoe [12]. On the soils studied by Arthur (1995), some analyses identified traces of fruits, nuts and cereals both burnt and fossilized, confirming the agricultural soil use [23].

The second hypothesis, linked to disposal site, is connected to the continuous use of the city: even after the collapse of the Roman Empire, the urban centers remained densely populated [21]. By an archaeological point of view, the study of the disposal sites in domestic context can be helpful to identify the housing conditions, to trace the behaviors [24] of people and to outline some aspects of their everyday life. The "waste" hypothesis was supported by Devos et al. (2013) [4], who found, into the DE soils, evidence of food and cooking waste, such as ash, charcoal, bones, charred seed and ceramics. These remains were commonly identified in European DE, so this hypothesis was also supported by Devos and Nicosia et al. (2012) [25]. In addition, Wouters et al. (2017) affirmed that the amount of charred peat, charcoal and remains of animals (e.g. fish) on the top of the DE stratus may be due to an increase of waste linked to human activities such as markets [19]. In the case studied by Wouters, it is possible to observe a transformation of the site from a rural one to an urban place,

over the Roman remains. In other papers, Devos supported the hypothesis of the DE as the result of waste accumulation, combining again charcoal with kitchen remains like burnt bones, eggshells, ceramics, seeds and ash [17]. Nicosia et al. (2019) also highlighted some aspects of the domestic conditions: the majority of the sites were characterized by the presence of *tuguria*, meaning that humans and animals, in particular farm animals, lived in the same space [26]. One of the causes of the absence of stratification in DE could be the re-mixing and re-arrangement of the domestic wastes accumulated on the floor [1].

Another hypothesis, promoted by Macphail and Country (1985) [27], is that DE was originated by re-arrangement of the organic and mineral materials deriving from perishable wooden structures, built and demolished by humans. This latter hypothesis is supported by the homogeneous appearance of the DE strata and also by Yule (1990) [28], who affirmed that the "re-arrangement" is the most credible hypothesis among the ones formulated so far.

Thanks to the high content of charcoal dispersed in them, DE seem to be very fertile soils in which it is possible to find evidence of ancient settlments and farming sites. Knowledge about the origin of DE could be helpful for developing innovative strategies and techniques for modern sustainable land use. In this sense, archaeology becomes "applied archaeology", that means the archaeological data are important to devolop new strategies for the future [29].

This fertility of soil was also discovered in the Amazonian region, where researchers found Anthropogenic soils.The archaeological DE found in Europe have many similiarities with Anthropogenic Dark Earth (ADE) or *Terra preta* (*de Indìo*)[30] found in South America. In particular, ADE are anthropic soils rich in carbon and, as DE, frequent evidence of past human activities is present. The radiocarbon analysis dated the soils to pre-columbian period [30], which can be related to the post-classic European DE. ADE was studied because of the high fertilizing power, as a model for sustainable agriculture in tropical environments, and for other land with a low nutrient capacity [31]. ADE presents a higher pH than average soils and higher cation exchange capacity. The ADE contains many nutrients from terrestrial and/or acquatic plants, human and animal excrements, bones and charcoal from incomplete combustion, just like European DE [32]. The fertilizing power aspect seems not to be correlated to the inorganic composition of the soil. The mineral composition of ADE is mainly represented by clay, iron and aluminium oxides, which means that the ADE ability of retaining nutrients depends on organic compounds. The ADE soils are rich in organic matter as a

consequence of the temperature of the equatorial area, that makes the organic decoposition faster [33]. The ADE black colour is mainly given by the charred material content, similarly to European DE. The Presence of ADE is an evidence of the worldwide diffusion of DE, that further underlines the importance of studying this phenomenon.

Figure 2.1: Normal Amazonian soil (left). The texture of these soils is loamy or sandy and the structure is dominated by stable micro-aggregates. The typical Terra Preta profile, the topsoils horizons have dark color and they can reach a depth up to 1 m (right) [31].

3 Historical context

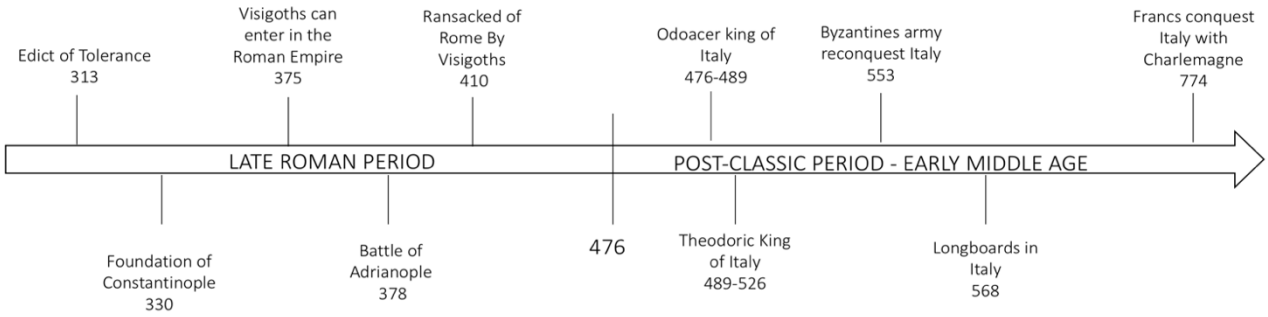

Figure 3.1: the main events occured during the Late Roman Period and the Early Middle Age

The post-classic period is a tumultuous period that starts during the last centuries of the Western Roman Empire and lasts until the early Middle Ages (between the 300 A.D. and the 700 A.D.). In figure 2.1 the main events occurred during the post-classic period are summarized.

In 313 A.D., the Emperor Constantin (306-337 A.D.) promulgated the Edict of Tolerance, where all the religions were accepted from the Roman Empire. The Christian persecution held formally.

During this period, the borders of the empires were weak and difficult to control, because the army was involved in other territories. For this reason, the northeastern boundaries were not strongly defended. From outside the Empire, in particular from the north-east, some Germanic populations pushed to enter the Empire.

In 370 A.D., the Huns subdued the Alans in the Caucasian region. Then they passed the Don river and found the Goth population. The Ostrogoths were subdued by the Huns, while the Visigoths, the other Goth population, moved until the Roman Boundary, the Danube river, asking to pass the borders and enter the Empire. In 375 A.D., the Visigoths were able to enter the Empire and they were designated in Thrace with a defensive aim. However, the Visigoths had no sustenance methods, and the Roman authorities did not help them. They became marauders and devastated the Balkan region. The reaction of the Roman empire took to the Battle of Adrianople in 378 A.D.

The barbarization of the army was at maximum level. This implicated many tensions in the administration of the Empire. Theodosius (378-395 A.D.) was the last Emperor that reigned on the two parts of the Roman Empire (the Western and the Eastern) together. After his death, the empire was divided and administrated by the two sons: Arcadius e Honorius. Honorius, assigned to the western part, was not able to defend Italy, so, the Visigoths rose up and easily arrived in Rome in 410 A.D. Under the command of Alaric, and they ransacked the city. In the following period, the Western Roman Empire was at the mercy of different barbarian populations. The Emperors were only instruments in the hands of generals, that tyrannized over the territories. In 476 A.D. Odoacer, king of the Goths, deposed the last emperor of the Western Roman empire Romulo Augustulus. Odoacer was crowned as the first King of Italy. This event marked the end of the Antiquity period [34].

Theodoric (474-526 A.D.), the king of Ostrogoths, also was *magister militum* (general) and he was allied with Eastern Roman Empire. In 489 A.D., the Ostrogoths won against Odoacer, and then Theodoric conquered all Italy [35], becoming its king.

During the mandate of Justinian (527-565 A.D.) in the Eastern Roman Empire, the emperor started a Greek-Gothic war in order to re-conquer the Western Roman Empire. The Ostrogoths were defeated in 553 A.D. by the byzantine army.

In 568 A.D., another barbarian population entered Italy: Longboards. They were from the Scandinavian peninsula. They arrived in Italy from Friuli Venezia Giulia region with Alboinus as leader. They conquered northern Italy and constituted their kingdom: the *Longobardia Major*. Then they

conquered also the southern part of Italy called *Longobardia Minor*. They settled in Italy until 774 when the Francs with Charlemagne won against Desiderius the last of the Longboard's king [35].

3.1 Relationship between Germanic migration and climate variations

The scientific research on the climatic reconstructions has made it possible to highlight the most important historic events as the result of climatic and environmental changes linked to civilization rises and collapses. Different analysis of the climatic and environmental conditions can be performed in order to detect the causes of the passage of different civilizations. For instance, the study of the difference of growth levels in the tree-rings [36], that shows the alternance between the season, reveals if a year was particularly cold or warm. The study of the rainfall, with precipitation reconstruction, can be helpful to underline anomalies in precipitations, showed significantly wet and dry summers [37]. Other information can be investigated from the study of chemical markers that reveals the differences in the vegetations during a particular period of time. For example the decrease of harvesting plants between the 3rd A.D. and 5th A.D. coincides with the largest European crisis: called the "*Migration Period"*, a period marked as long-term political disorder, cultural variation, and socio-economic instability [38]. The "*Migration Period"* is the period in which the Germanic population started to move from the north to the south. Probably this migration stated from the Huns that in the north-east of the Asia moved to European lands, according to climate change. The Huns left their lands and move towards the south. The other population, that they met, began the same migration for two motives: one the Huns, that invaded other barbarian populations, and the other one the climate variations. The climate changes did not affect only once in the history but there is wide evidence of the correlation between big migratory periods and climatic variations. Two decreases of the summer temperature coincide with the Celtic Expansion (350 B.C.) and the Roman Conquest (50 B.C.). According to the study of Büntgen et al. 2011 [38] the *Migration Period* is linked with a climate change.

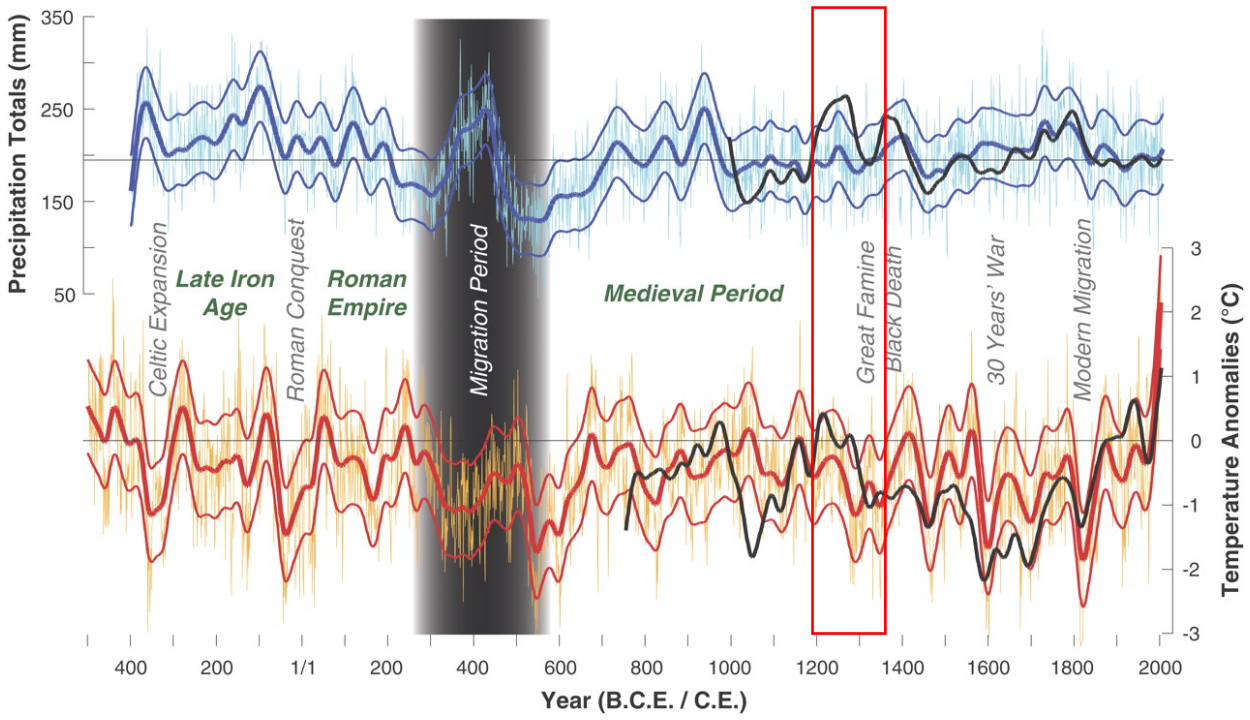

Figure 3.2: Graph of variation in temperature and precipitations related to human history[38].

As shown in figure 3.2, the *migration period*, centered between the 3rd and 4th century, the temperatures present anomalies (temperature decreased and rainfall increased) in correspondence with a period of serious crisis in the Western Roman Empire, political disorder, and economic trouble in several provinces [39,40]. In addition, the barbarian invasion from the north occurred. Precipitation increased during the reconquest of the Western Empire (4th century) with Constantine and Valentinian, while precipitation decreased during the end of the Western Roman Empire in the 5th century. Then, again, precipitation decreased sharply in the first half of the 6th century. During the second half of 6th century the Justinian Plague developed from the eastern Mediterranean [41]. During this period, a sudden variation in temperature and rainfall occurred.

Spring precipitation and summer temperature began to increase from the end of 6th and the beginning of 7th century. The start of wetter and warmer summers is concomitant with the consolidation of new kingdoms in the past Western Roman Empire [42].

Wet and warm summers paralleled the rapid cultural and political growth of medieval Europe under the Merovingian and Carolingian period [38].

Quick climate changes, together with epidemics, had the capacity to compromise the development of agrarian cultures. Unfavorable climate conditions, such as frequent rainfalls and colder temperatures, may have played a role in the diffusion of famine before the Black Death plague. The

climatic conditions, the famine and the consequent plague reduced the central European population dramatically (see the red rectangle in figure 3.2) [38,41].

The association of climatic variation with settlement desertion in Europe may provide a response to the problem of Germanic migrations during the last Roman Empire centuries (in *Migration Period)*. Climatic change, together with the internal problems of the Empire, may be the major cause of the Western Roman Empire collapse [38].

4 Chemical Markers

Chemical markers are specific substances employed in order to reconstruct the changes and phenomena happened during the stratification of soils. This aim is to define the origin and what are the main components of the DE. Through the study of the markers, it is possible to trace environmental changes and human activities that affected the studying site.

The markers analyzed for this research are anhydrous monosaccharides (AMs), polycyclic aromatic hydrocarbons (PAHs), *n*-alkanes, fecal, plant and fungal sterols (FPFS) and miliacin. Each analyte provides different information useful to characterize the samples. In addition, charcoal fragments have been detected as result of organic matter combustion.

The vertical growth of urban stratifications is considered as associated to the social and historical evolution of that site. Typical organic and inorganic markers inside the archaeological stratifications can be used to assess the presence of vegetation and the environmental conditions. In addition, various information about agricultural practices, animal livestock can be gathered. Through the reconstruction of chemical markers, it is possible to reconstruct the presence of humans and their activities.

Previous studies, for instance, focused on the miliacin detection in soils, derived from the cultivation of millet, not only for human consumption, but also as food for animals. Therefore, miliacin was also used as evidence of livestock breeding [43–45]. Sterols can be used to reveal the presence of ruminants, and so they can be useful to trace ancient pastoral practices, and the presence of animals and humans[45]. Other information can be obtained from the reconstruction of past environmental conditions detecting markers such as *n*-alkanes, polycyclic aromatic hydrocarbons (PAHs) and anhydrous monosaccharides (AMs). These markers are indicators of vegetation and fire events (PAHs

and AMs) [45,46]. In this way, the analytical approach on soil stratifications can be interpreted from a historical and archaeological point of view, revealing past everyday life aspects [1].

4.1 Detection of fire events

The Dark Earth are soils linked with human activities and therefore also with fires. The biomass burning products can represent an evidence of human presence. One of the hypotheses on the origin of DE is related to the accumulation of domestic waste including charred material [27,47]. For this reason, markers related to biomass burning were here analyzed. In particular, the species investigated to reconstruct past fire events are charcoal, PAHs and anhydrous monosaccharides. The analysis of fire events can be related with the human presence, above all in an urban context. For this reason, three sets of markers coming from biomass burning were considered. These markers give complementary information about the entity, the origin and the duration of the fire event.

4.1.1 Charcoal

Charred materials are the products of incomplete combustion of vegetation [48]. Charcoal typically has a high carbon content (60–90%), a proportion of which is in a highly condensed aromatic molecular configuration [49,50]. Macro molecules of charcoal generally preserve information about its origin [51]. Charcoal is a very stable marker, for this reason it preserves its characteristics for long time and it accumulates into sedimentary sequences [52,53]. Charcoal is produced by fire, in general it results from the incomplete combustion of plants and animals, particularly invertebrates [54]. During the burning process pyrolysis reactions occur, plants are subjected to rapid high temperature heating that causes the breakdown of cellulose in plant tissues [55]. The pyrolysis reaction starts when the heat of the fire enters in the plant tissues where oxygen is poor (charring front). During this process, heat breaks the molecules emitting volatile gasses that outflow and when they meet oxygen, they burn [55]. If this reaction is stopped at incomplete combustion the charcoal is obtained in form of residue. In wildfires it is not possible for large plant to become completely charred: the surface layers of the tree will combust primarily, the inner part will not become charcoal [56].

4.1.2 Polycyclic Aromatic Hydrocarbons

PAHs are originated by combustion of plants or fossil fuels. From different sources different analytes are produced, for this reason trough the analysis of PAHs it is possible to reconstruct the origin of the burning products. The main difference is between the vegetal and petrogenic origin [57,58]. PAHs are constituted by two or more conjugated aromatic rings: this structure makes PAHs very stable molecules, and for this reason they are investigated in order to reconstruct also very old fire events [45,58].

The variation of temperature, heating intensity, aeration, duration of smoldering and flaming conditions determine the accumulation of different PAHs. Starting from the weight of the PAHs detected, it is possible to identify the dimension of fire events [57]. PAHs are formed when the burning temperature increases over 400 °C. In particular, low molecular weight (LMW) PAHs are synthesized around 400 °C, medium molecular weight (MMW) PAHs occur starting from 500 °C and high molecular weight (HMW) congeners appear between 600-650 °C [59]. The LMW PAHs are lighter, more water soluble and more perishable than the heavier congeners. These aspects make them less informative of a specific site, since they can easily degrade and cover long distances through atmospheric transport. The MMW and HMW, on the contrary, are heavier and tend to deposit closer to the source and be associated to medium to coarse sized particulates, therefore they are more characteristic of the site [59].

Among the compounds considered here, the PAHs produced by biomass burning are mainly: phenanthrene, anthracene, fluoranthene, pyrene, benzo(a)anthracene and benzo(a)pyrene [57]. When shrubs, herbaceous and gramineous plants burn, characteristic PAHs like phenanthrene, fluorene and pyrene are produced [57]. The PAH structures analyzed in the present work are shown in figure 4.1.

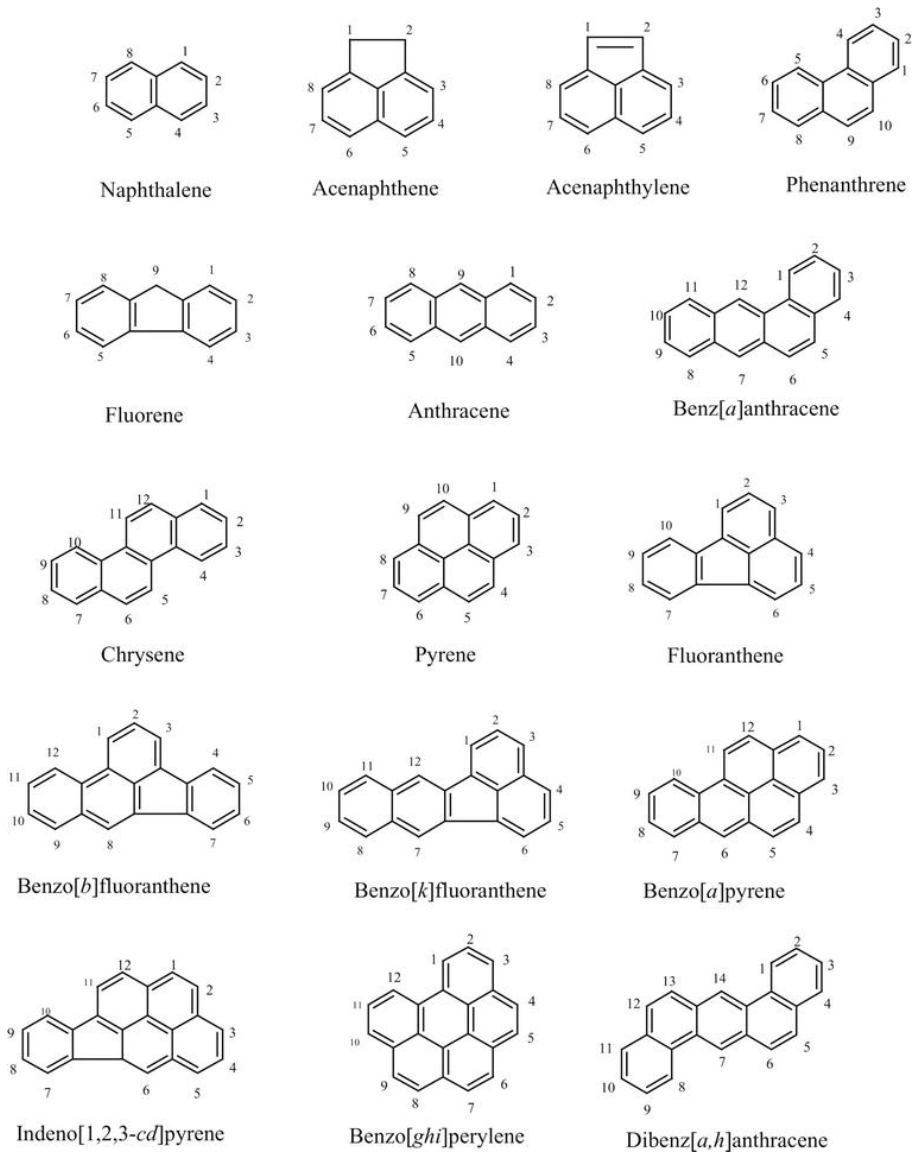

Figure 4.1: Polycyclic Aromatic Hydrocarbon structures [intechnopen.com].

4.1.3 Anhydrous monosaccharides

The biopolymers are the main components, in addition to water, of plant species. The biopolymers mainly present are cellulose and hemicellulose, and also lignin. These polymers are present in different quantities in each vegetal species [60]. Cellulose is composed by β-D-glucopyranose with packed structure ensured by hydrogen interaction. The hemicellulose is composed by sugars such as arabinose, mannose, galactose, xylose and glucose, forming molecules by 100-200 units. The lignin is originated by alcohol polymerization, in particular of coumaryl, coniferyl and synapil alcohols. The three biopolymers are the main constituents of the cellular wall [61], for all the vegetal species. Levoglucosan (1,6-anydrous-β-D-glucopyranose) is one of the products of the thermal degradation

of cellulose: the levoglucosan production starts when the burning temperature is higher than 300°C [57]. Mannosan (1,6-anhydrous-β-D-mannopyranose) and galactosan (1,6-anhydrous-β-D-galactopyranose) are two isomers of levoglucosan. These three molecules were quantified in the present work. Mannosan and galactosan are produced by the thermal degradation of hemicellulose. It is possible, through the detection of anhydrous monosaccharides, to reconstruct the entity and the type of fire events that occurred in an area [62]. Simoneit [63] affirms that levoglucosan is formed only from the thermal degradation of cellulose, for this reason it is a good marker for the reconstruction of biomass burning events. It is important to notice that mannosan and galactosan can be affected by the temperature of fire and by the prolonged exposition to it. In fact, prolonged fire conditions can degrade the two isomers, that can be more difficult to detect [64]. Figure 4.2 shows the anhydrous monosaccharides analyzed in this thesis.

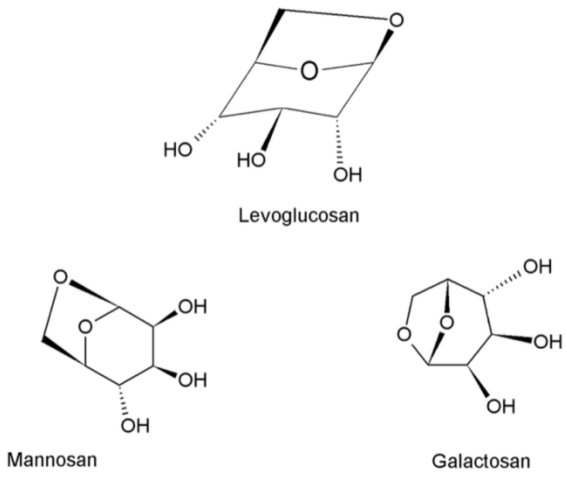

Figure 4.2: Levoglucosan, mannosan and galactosan molecules[65].

4.2 *n*-Alkanes

The *n*-alkanes are detected in order to reconstruct the local vegetation and the environmental conditions. In the case of the DE, the *n*-alkanes are investigated to trace the vegetation present in the archeological site, but above all to confirm if the site was used for agricultural purposes. The *n*-alkanes are among the main components involved in the biosynthesis of vegetal organisms and microbes [66]. The results of the biosynthesis are aliphatic hydrocarbons that constitute the plant cuticle, that is the surface layer used in order to protect the plant from external agents. This layer is

a hydrophobic barrier used to maintain the humidity equilibrium. The different distribution of hydrocarbon chains is characteristic of plant species [45,67]. Plants produce mainly odd chains of carbon, if this predominance is absent probably is because there was a strong reworking of the soil, or probably there was many bacterial actives [66,67].

The *n*-alkanes can be classified trough the length of the carbon chains. The shorter chains derive from algae, bacteria and plankton (chains lower that 20 carbon atoms). The medium length (between 20 and 25 carbon atoms) arise from aquatic plants. The longer carbon chains (between 25 and 35 carbon atoms) are representative of terrestrial plants [68]. The terrestrial plants can be also classified between arboreal and herbaceous plants, in particular the arboreal typically have 27 and 29 carbon chains, while herbaceous have 31 and 33 carbon chains [66]. In addition, these markers are affected by the environmental conditions of the surrounding area. From the same plant, the production of different *n*-alkanes could be the result of a climatic variation, because the plant is subjected to climate variation that could effected its production of *n*-alkanes [69].

4.3 Human presence

The Dark Earths are strictly connected to the human presence, also because they have been found only in urban context. For this reason, DE are themselves an evidence of human presence, but it is necessary to try to identify their origin. To detect human and animal presence, sterols can be employed. Moreover, miliacin has been investigated to reconstruct the agricultural practices of the post-classic period.

4.3.1 Miliacin

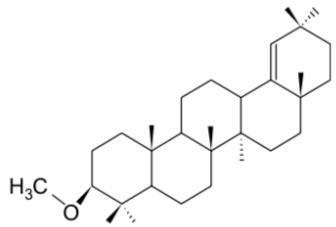

Figure 4.3: Miliacin molecule[44]

Miliacin (figure 4.3) is a pentacyclic triterpene, with 30 atoms of carbon arranged in five rings. This molecule is a constituent of broomcorn millet (Poaceae), in particular it is a major component of *Panicum miliaceum.* The broomcorn millet is not an indigenous plant in Europe, but it was introduced

from Asia, in middle Bronze age (~ 1800 B.C.), and so has miliacin [45,70]. Broomcorn millet has a long history, in Northern Italy there is evidence of the cultivation of the millet since the Bronze and Iron Age [43,71]. During the Roman period, millet was nothing more than a minor crop. Most historical reports suggest that, apart from animal feed, it was considered suitable only for the poor people [71]. Another evidence of millet consumption by lower social classes is related to the fact that millet was exempt from taxes in Europe during the middle ages [71]. For this reason, it is common to detect miliacin and millet remains in an urban context. The presence of miliacin in agricultural soils, in high concentrations, proves that millet was locally cultivated and not imported from other countries [43,45].

4.3.2 Fecal, plant and fungal sterols

Fecal and plant sterols are important markers used in order to detect animal presence and in particular the presence of human beings [72]. Also, trough the sterols investigation it is possible to distinguish between animal and vegetal provenance, in order to collect information about agricultural and livestock practice. These molecules are stable, so it is possible to detect them in very old sediments, as far back as 10,000 years [72]. By detecting fecal sterols, it is possible to obtain information about the origin of the Dark Earth, for example their detection can be related to the presence of disposal sites, in which waste was collected and accumulated [27]. In the intestine of mammals a reaction occurs, mediated by bacteria, obtaining 5β-stanol (5β-colestan-3β-ol for omnivorous, 5β-stigman-3β-ol for the herbivores) from Δ^5-sterol [73,74] .

In the human feces, the sterol mainly present is 5β-colestan-3β-ol (coprostanol) its epimerous the epicoprostanol (5β-colestan-3α-ol [72]. Also vegetal species produce sterols, their marker is β-sitosterol [46,74,75]. The stigmastanol is the main product of the β-sitosterol reduction. This reduction can occur in the digestive system of the ruminants, for this reason stigmastanol is also a marker for the presence of livestock, also associated to human activity [45]. Ergosterol (ergosta-5,7,22-trien-3β-ol or 24R-methyl-cholesta-5,7,22(E)-trienol) is a sterol found solely into the fungal cell membrane. It has same function as cholesterol in animals (cholesterol forms the cell membrane and is also the first component of hormones and bile acids) so it is fundamental for fungal life [76]. Figure 4.4 shows the sterols analyzed in this thesis.

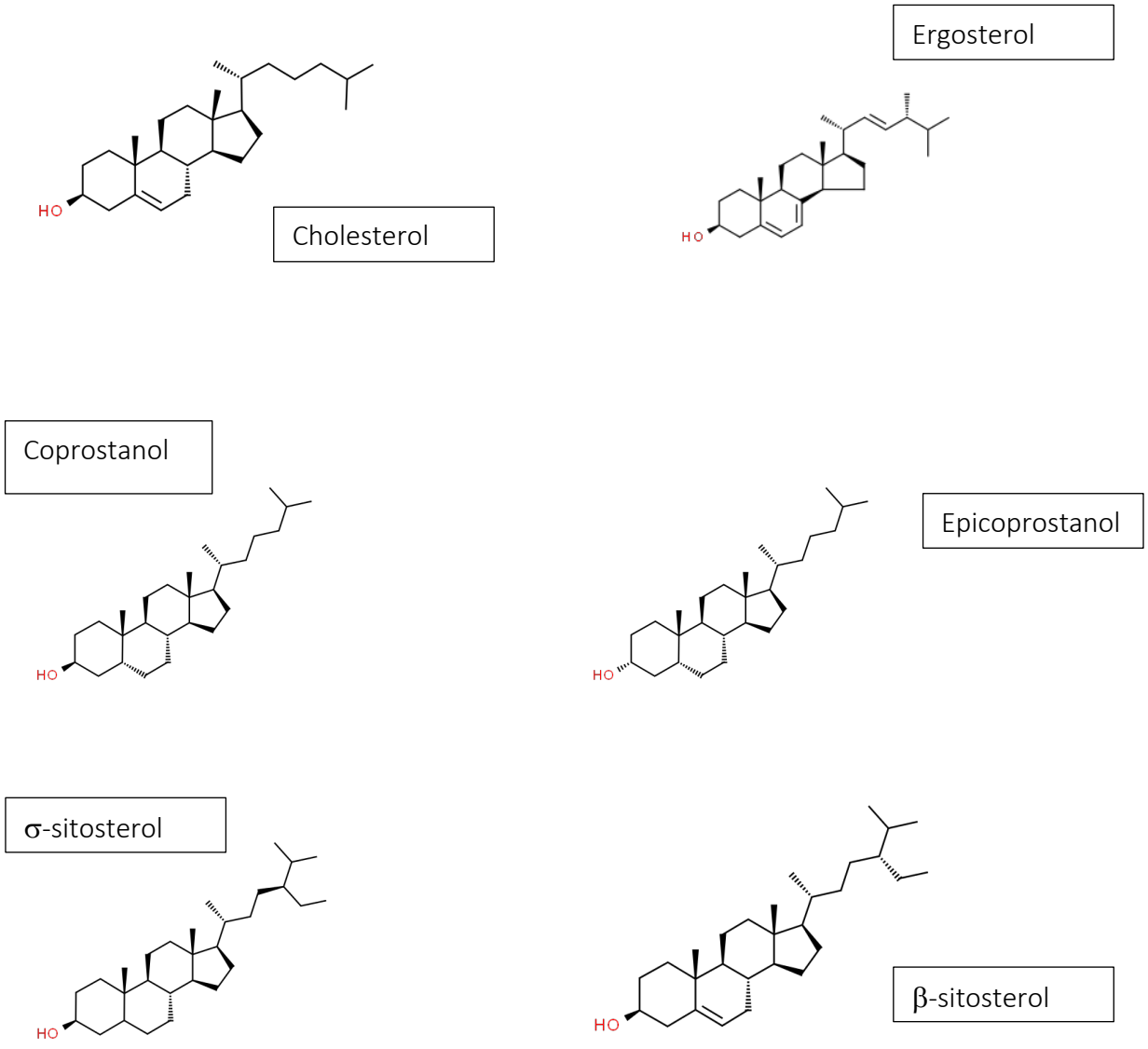

Figure 4.4: sterols molecules [chemspider.com]

5 MATERIALS AND METHODS

In this part, the preparation procedure from the raw sample to the analysis will be presented. In addition, the chapter describes the techniques used to perform the investigation. A summary of the techniques employed, and the analytical process is provided in *fig. 5.1*.

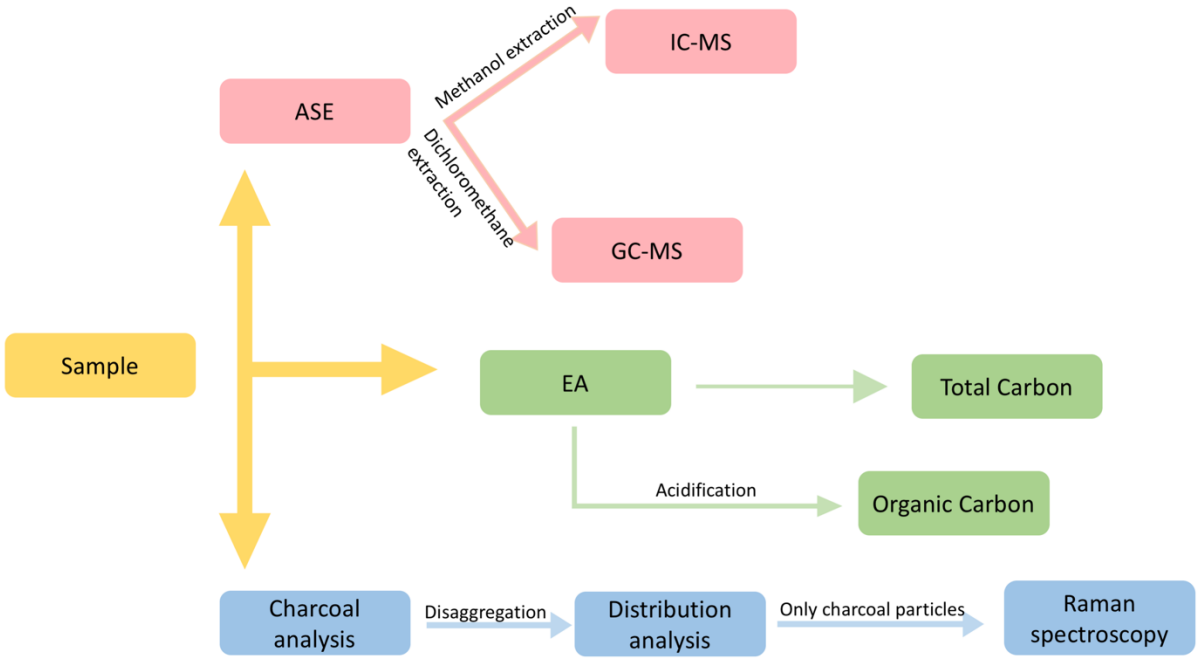

Figure 5.1:block diagram of sample treatments.

5.1 Standards and reagents

The solvents employed to carry out the analysis were pesticide grade solvents, in particular methanol (MeOH), dichloromethane (DCM), *n*-hexane (Hex) and 2,2,4 trimethylpentane, from Romil Ldt. The solvents were used, also, for the decontamination of glassware. Anhydrous Na_2So_4(≥ 99%, from Sigma Aldrich, Saint Luis, USA), previously oven-dried at 150°C for 24h and then washed with DCM and Hex, was employed to prevent accumulation of water in the sample during treatment. N,O-Bis(trimethylsilyl)trifluoroacetamide with 1% of trimethylchlorosilane(BSTFA 1% TMCS, Sigma Aldrich) was used as derivatization agent. A 10% of aqueous solution of $(NaPO_4)_6$ (Sigma Aldrich) was used as disaggregation agent for charcoal analysis.

The standards employed for the quantification of analytes were:

- Hexatriacontane($C_{36}H_{74}$), from Sigma Aldrich, in 2,2,4 trimethylpentane.
- Isotope-labeled polycyclic aromatic hydrocarbons:$^{13}C_6$-acenaphtylene,$^{13}C_6$-phenanthrene,$^{13}C_4$-benzo(a)pyrene, from Sigma Aldrich, from Cambridge Isotope Laboratories (CIL, MA, USA) in DCM.
- 5α-androstane, from Sigma Aldrich, in DCM.
- Isotope-labeled cholesterol-25,26,27-$^{13}C_6$, from Sigma Aldrich, in DCM.
- Isotope-labeled levoglucosan from CIL, in ultrapure water.

5.2 Sampling site

In this project, three archeological sites from the north-east of Italy, in particular from Veneto region, were considered. Two of these sites are located in the city center of Verona and one in Mel (BL). The samples were provided by Dr. Cristiano Nicosia (Department of Cultural Heritage, University of Padua).

5.2.1 Verona

The two sites in Verona were *Via Pigna* (VP) (*fig.5.2*) and *Vicolo San Pietro in Monastero* (SPM) (*fig.5.3*), adjacent to each other. During restoration works, archeologists found the remains of two ancient urban sites, dating back to the post-classic period.

Figure 5.2: General view of Via Pigna site. It is possible to see the difference between normal soils and the Dark Earth that has basically darker color. [C. Nicosia]

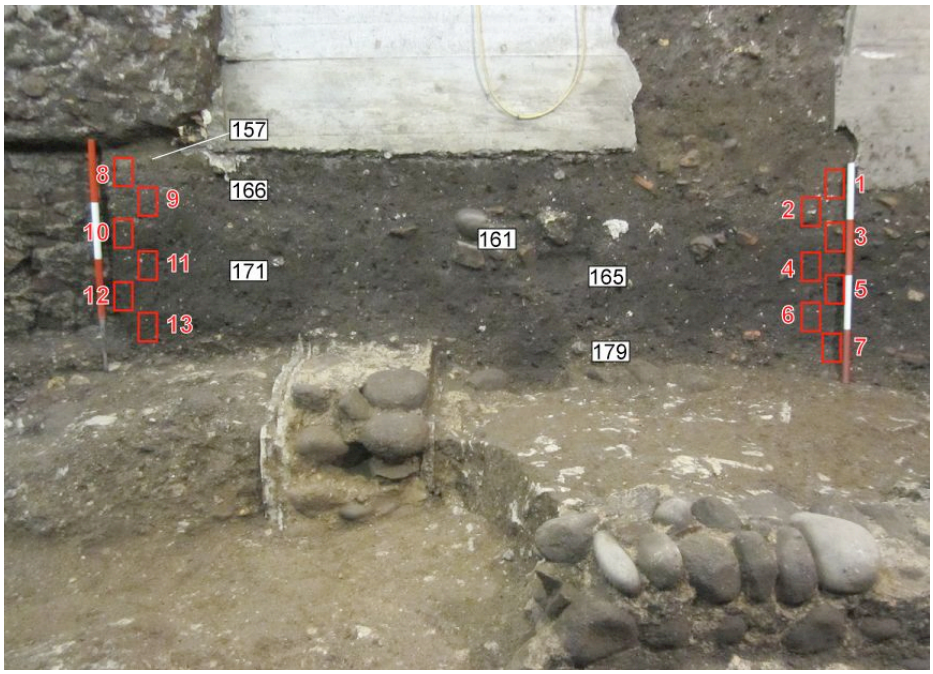

Figure 5.3:Sampling sites of Vicolo San Pietro in Monastero. The figure points out the difference between the Dark Earth zone, in the center of the photo, from normal soil, the separation is very identifiable. [C. Nicosia]

The SPM stratification is around 80 cm high, the samples were collected from two different parts of the same stratification opposite to each other, as shown in figure 5.2. VP samples were collected in two different parts of the same stratification which is 30 cm high.

The samples were cut in the form of bricks ~9x9 cm in order to obtain thin sections for the future morphological investigations. From each sample, two aliquots of ~20 g were collected to perform all the analysis included in this work. The upper part and the lower part were stored separately. After the collection, the samples were dried in the oven at 30 °C until constant weight. The samples were generally dark colored. In particular, the SPM were greyish, while the VP were darker, except for the VP_3 that had a more reddish color, probably because a brick was embedded in it.

5.2.2 Mel

Mel is a city in the province of Belluno, located in the northern part of Veneto region. The excavation was performed as preventive archaeology during restoration works on a building (*fig.5.4*).

Figure 5.4: Sampling sites of Mel (BL). [C. Nicosia]

The MEL stratification is around 30 cm high. The samples were collected in four parts of the stratification as shown in fig. 5.4. The samples were in bulk form, so it is not possible to distinguish the top from the bottom. The samples were dark and very wet, so it was necessary to dry them to constant weight as described above.

5.3 Instrumental equipment and procedure

5.3.1 Extraction and volume reduction

The extraction of samples is performed with the Accelerated Solvent Extraction (Dionex Thermo Fisher ASE 350). The extractor works performing a solid-liquid extraction at high temperature and pressure. Aliquots of each sample were extracted with MeOH for the analysis of monosaccharide anhydrides and with DCM for all the other compounds. 22 mL stainless steel cells were employed by filling each with 1-5 g of sample dispersed in diatomaceous earth, previously decontaminated in the muffle furnace, and ~2 g of anhydrous Na_2SO_4.

The cell is filled with the extraction solvent, then brought to 100 °C (MeOH) or 150 °C (DCM) and 1500 psi for 5 minutes (static phase). At the end of the cycle, the instrument drains the product of the extraction in a pre-cleaned 60 mL glass vial. The cycle is repeated twice for each sample and blank, in order to maximize the transfer of analytes to the liquid phase.

Before starting the extraction, the standard solutions, previously prepared, are added to samples and blanks in order to allow quantification through the isotopic dilution method (*tab.5.1*).

Table 5.1: internal standards used to quantify the analytes.

Standard	Detection of	Concentration	Quantity
Isotope-labeled levoglucosan	Anhydrous monosaccharides	5ng μL^{-1}	20 µL
Hexatriacontane ($C_{36}H_{74}$)	*n*-alkanes	50 ng μL^{-1}	50 µL
Isotope-labeled polycyclic aromatic hydrocarbons	PAHs	1 ng μL^{-1}	50 µL
5α-androstane	Miliacin molecule	10 ng μL^{-1}	50 µL
Isotope-labeled cholesterol-25,26,27-$^{13}C_6$	Fecal and plants sterols	10 ng μL^{-1}	20 µL

Several blanks were processed together with samples (one blank every five samples). Blanks were prepared with diatomaceous earth, Na_2SO_4 and internal standards employed in the extraction.
At the end of extraction, the cells were washed carefully a 2-5% Contrad solution, then rinsed, dried and cleaned in the ultrasonic bath with MeOH, DCM and Hex.
DCM extracts were concentrated to ~200 µL. The *Turbovap II,* from Caliper Life Science, was used for volume reduction. The instrument employs a thermostatic bath set at 23 °C and a flux of nitrogen dispensed by nozzles in glass tubes containing the extracts. Volume-reduced samples were transferred into gas chromatography vials and stored in the refrigerator until analysis.
MeOH extracts were concentrated to dryness at 35 °C and redissolved in 500 µL of ultrapure water, then filtered onto PTFE 0.45 µm syringe filters. The samples were transferred into ion chromatography vials and stored in the freezer until analysis.

5.3.2 Chromatographic analysis

The two different extracts (MeOH and DCM) were analyzed as follows by ion chromatography gas chromatography, respectively, both coupled to single quadrupole mass spectrometry.

5.3.2.1 Ion chromatography – mass spectrometry (IC-MS)

This technique was used to separate and quantify levoglucosan, mannosan and galactosan in the MeOH extract. Ion chromatography is a liquid chromatography based on the different affinity between a mobile phase and a stationary phase. The technique separates the ions in the sample according to the charge and the steric hindrance. The charge competition, created between the ion and the stationary phase, takes to the split of analyte in order to perform chromatography investigation. The chromatography separation is carried out by a Dionex Thermo Fisher ICS 5000ion chromatograph, coupled with an *MSQ plus* (Thermo Fisher Scientific) quadrupole mass detector. The *CarboPac*^{TM} MA1 column (ethyl-methylbenzene 55% anddivinylbenzene, 2 x 250 mm, Thermo Fisher Scientific) is employed to perform the analysis. A guard column (*AminoTrap*^{TM}*,* 2x250 mm,Thermo Fisher Scientific), made in polymeric resin, was used in order to prevent aminoacidic interference during the analysis. The stationary phase is made with a solution of NaOH provided by an eluent generator. The eluent generator guarantees the reproducibility on the preparation of solution. The flux was 250 µL min^{-1}. The sample injection volume was 50 µL.

The elution gradient was as follows: 20 mM from 0 to 30 min, 100 mM between 30 and 45 min (wash phase), then the mobile phase is carried to the initial concentration of 20 mM between 45 and 55 min. The mobile phase is eliminated by a suppressor (*ASRS 500*, 2 mm, Thermo Fisher Scientific). After the column, a7‰ ammonia solution in MeOH (at 0.025 mL min^{-1}) is added in order to increase the volatility of the solvent in the source and obtain a better ionization of the analytes. The ionization was achieved through an *electrospray* source (ESI) that works at high pressure (2000 psi) operating in the negative mode. Identification and quantification of compounds were performed through single quadrupole analysis in Selected Ion Monitoring (SIM) mode (*tab.2.2*).

5.3.2.2 Gas Chromatography-Mass Spectrometry (GC-MS)

Gas chromatography coupled with a mass spectrometer was employed to determine *n*-alkanes, polycyclic aromatic hydrocarbons (PAHs), miliacin and sterols.

The system is equipped with an Agilent Technologies 7890A GC System coupled with an Agilent Technologies 5975C inert MSD detector. The capillary column used for the analysis is an Agilent Technologies HP5-MS (60 m, 0.25 inner diameter, 25 µm film thickness). The mobile phase is 5% phenyl-methylpolysilossane.

Based on the different affinity with the capillary column and the temperature program, the analytes come out at different retention times, and subsequently fragmented in the electron impact source (70 eV at 230 °C). The ions, positively charged, are pushed through the quadrupole where the different mass/charge ratios allow compound identification in SIM mode (*tab.2.2*).

The chromatographic methods employed to separate the different classes of analytes were as follows:

- *n*-alkanes: initial temperature 150 °C (1 min), 18 °C min^{-1} to 315 °C (16 min). Post-run: 15 minutes at 315 °C. The injection is performed in *splitless* mode at 300 °C (split valve open 1 min from injection at 50 ml min^{-1}). The carrier gas is He, with a flux of 1.2 mL min^{-1}.
- Polycyclic Aromatic Compound (PAH): initial temperature 70 °C (1.5 min), 10 °C min^{-1} to 150 °C (10 min), 3 °C min^{-1} to 300°C (15 min). Post-run: 30 min at 305 °C. The injection is performed in *splitless* mode at 300 °C (split valve open 1 min from injection at 50 ml min^{-1}). The carrier gas is He with a constant flux of 1 mL min^{-1}.
- Miliacin: initial temperature 100 °C (1min). 30 °C min^{-1} to 315 °C (12 min). Post-run: 10 min at 315 °C. The injection is performed at 300°C, in *splitless* mode with the split valve opened 1 min after injection. The carrier gas is He with a constant flux of 1.2 mL min^{-1}.

After the analysis of polar compounds, the samples are derivatized in order to analyze sterols. 100 µL of BSTFA with 1% TMCS are added to the samples. Then the samples are heated in a thermoblock at 70 °C for 60 min and analyzed after 24 hours.

The chromatographic separation of fecal and plant sterols is performed as follows:

- initial temperature 150 °C (1 min), 30 °C min^{-1} to 220 °C, 2 °C min^{-1} to 300 °C (6 min). Post-run: 20 min at 315 °C. The carrier gas (helium) has a flux of 1 mL min^{-1} and the injection is run at the temperature of 280 °C, *splitless* with the split valve open 90 seconds after the injection.

The table 5.2 presents the mass charge ratios used for the SIM determination

Table 5.2: Molecular ions used for SIM determination

Molecules	m/z

Anhydrous monosaccharide	
Levoglucosan -$^{13}C_6$	167
Levoglucosan	161
Mannosan	161
Galactosan	161
n-alkanes	
C_{10}-C_{36}	71; 99; 85; 113
PAHs	
Naphthalene	128
Acenaphthylene	152
Acenaphthene	154
Acenaphthylene - $^{13}C_6$	158
Fluorene	166
Phenanthrene	178
Anthracene	178
Phenanthrene- $^{13}C_6$	*184*
Fluoranthene	202
Pyrene	202
Benzo(a)anthracene	228
Rethene	234
Benzo(b)fluoranthene	252
Benzo(k)fluoranthene	252
Benzo(e)pyrene	252
Benzo(a)pyrene	252
Perylene	252
Benzo(a)pyrene -$^{13}C_6$	*256*
Benzo(g,h,i)perylene	276
Indenol(1,2,3,c,d)pyrene	276
Dibenzo(a,h)anthracene	278
Miliacin	
Miliacin	177, 189, 204, 425, 440

5α-androstane- $^{13}C_6$	245, 260
Sterols	
Coprostarol	215
Epicoprostanol	370
Cholesterol	368; 370
Cholesterol- $^{13}C_6$	332; 371
Cholestanol	335; 460
β-sitosterol	396
σ- sitosterol	473

The results obtained from the GC-MS analysis were elaborated with the Chemstation Data Analysis software to integrate peaks and allow the quantification of the analytes. In particular the internal standard method was used to quantify the analytes, then the results were calculated through response factor, and corrected with blank subtraction. The response factor (RF) is a solution containing all analytes and internal standards in a known concentration, injected several times together with the samples in order to control the instrument response and correct the quantification as described below:

$$\frac{A_n}{A_{is}} \bullet \frac{C_{is}}{C_n} = RF$$

$$\frac{A_a}{A_{is}} \bullet \frac{Q_{is}}{RF} = Q_a$$

$$Q_a - Q_b = Q_{ae}$$

$$\frac{Q_{ae}}{sample\ weight} = C_{ae}$$

A: area

C: concentration

n: native compound

is: internal standard

RF: response factor

a: analyte

b: blank

Q: absolute quantity

Q_{ae}: absolute quantity after blank subtraction

5.4 Elemental Analyzer

The *elemental analyzer* (EA) is an instrument used to investigate elemental species like carbon, nitrogen, oxygen, and hydrogen in order to characterize the composition of samples. The EA is composed by a furnace and a reactor, followed by a capillary column that separates the gases developed from sample combustion. At the end there is a thermal conductivity detector (TCD) that detects the different species. The reactor is made with a quartz tube, filled with silver/cobalt (AgCo) to eliminates the sulfur gases, metal copper (Cu) used in order to reduce all the gases, and chromium oxide (Cr_2O_3) at the end to achieve complete oxidation. Helium is the carrier gas, while oxygen is used during sample combustion.

In this work, the EA was used to quantify total and organic carbon. The samples are ground and weighed into two aliquots. Then, one of the two undergoes a process of acidification (aimed at eliminating inorganic carbon) by adding a 10% HCl solution until completion of the reaction. This samples are washed with distilled water and centrifuged until the pH resulted neutral, and finally dried in the oven at 30 °C.

Acidified and non-acidified samples are weighed (~0.2 mg) and closed in small tin capsules. Each sample is analyzed in three replicates both for total carbon and for organic carbon. Several blanks (empty capsules) and standards for instrument calibration where prepared as well. The standard is acetanilide, from Thermo Fischer Scientific. The method employed for total carbon analysis is the following: furnace temperature 950 °C, column temperature 75 °C, carrier gas at 120 mL min^{-1}, oxygen flux at 250 mL min^{-1}.

5.4.1 Charcoal analysis

Three aliquots of each samples are weighed (~0.5 g) and stored in plastic beakers. 50 mL of a 10% solution of $(NaPO_4)_6$ are added directly to the sample, together with 50 mL of commercial bleach in order to disaggregate and dissolve part of the matrix, as described by Whitlock and Larsen (2001)[48]. The resulting material was sieved in fine mesh sieves (1 mm, 500 µm, 250µm, 125µm and 63 µm).

Each size fraction obtained was stored in distilled water, before being transferred to a plastic Petri dish and observed with the stereomicroscope. During this phase, the charcoal particles were counted to obtain a size distribution analysis.

The microscope used for the analysis is an Olympus SZ61 TR with integrated camera C-mount with 0.5X lens built in, supported by quick operator DP20-5E. The microscope supports 0.67X to 4.5X magnification, working distance of 110mm, objective M48 thread x 0.75. The images were acquired by Cell* imaging software for Life Science Microscopy by Olympus.

6 RESULTS

Results will be presented based on the sampling site and therefore divided into the two macro areas of Verona and Belluno.

6.1 Verona: Vicolo San Pietro in Monastero (SPM)

6.1.1 Total and organic carbon

The carbon content in the samples was measured both as total carbon and as organic carbon, after acidification. The latter represents the amount of carbon related to the input of organic matter to the site.

The total and organic carbon contents, for the two sampling points SPM_A and SPM_B, are given as percent amount (fig. 6.1). The total carbon for SPM_A ranges between 4.2 % and 8.6 %, the average value is 6.1 % ± 1.9 %. The organic carbon for the same sampling site ranges between 2.8 % and 5.7 %, with an average value of 4 % ± 1.2 %.

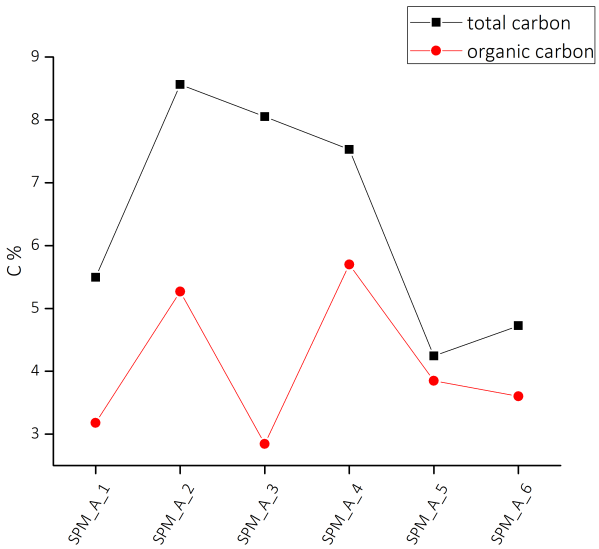

Figure 6.1: Total and organic carbon content in SPM_A samples.

The total carbon for SPM_B ranges between 2.5 % and 8.3 %, the average value is 5.4 % ± 1.5 %. The organic carbon for the same sampling site ranges between 1.9 % and 8.1 %, the average values is 3.2 % ± 0.6 %. Figure 6.2 shows the percent amount of total and organic carbon in SPM_B.

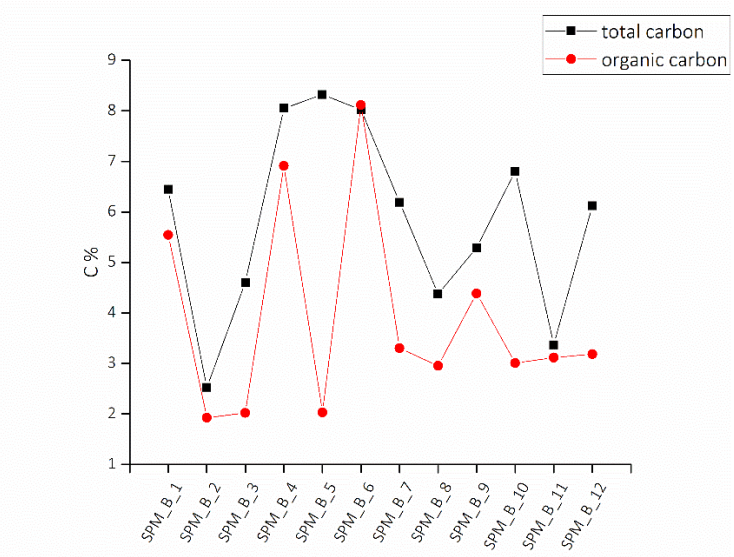

Figure 6.2: Total and organic carbon content in SPM_B.

6.1.2 Polycyclic Aromatics Hydrocarbons (PAHs)

PAHs were divided into three classes, according to the molecular weight. In particular, PAHs with 2 or 3 aromatic rings are regarded as low molecular weight (LMW) compounds, medium molecular weight (MMW) PAHs are compounds with 4 aromatic rings, while high molecular weight (HMW) PAHs are the ones with 5 or 6 aromatic rings.

One of the dominant factors in the formation of PAHs is related to the temperature (as discussed in paragraph 1.3): in particular, the number of aromatic rings increases with temperature. Also, the type of fuel (e.g. arboreal or herbaceous) is a discriminating variable for their formation, as a consequence of the temperature and duration of the combustion sustained [59].

The sum of PAHs is presented as LMW, MMW and HMW for both profile sampling site SPM_A and SPM_B. Table 6.1 summarizes PAH values the range values, the mean values and variance coefficient for each sampling site.

Table 6.1: Results of PAHs from SPM_A and SPM_B

		LMW	MMW	HMW
SPM_A (ng g^{-1})	Minimum value	0.43	8.8	1.9
	Maximum value	7.1	77.7	90.1
	Number of samples	6	6	6
	Average value	3.1	29.9	34.2

	Standard deviation	2.9	28.4	38.8
	Coefficient of variation (%)	93%	94%	114%
SPM_B (ng g^{-1})	Minimum value	0.81	1.1	3.9
	Maximum value	10	87.7	218.4
	Number of samples	12	12	12
	Average value	4.7	34.5	42.7
	Standard deviation	3.2	25.8	60.1
	Coefficient of variation (%)	68%	74%	137%

Figures 6.3 and 6.4 show the LMW, MMW and HMW PAH concentrations in samples from SPM_A and SPM_B respectively.

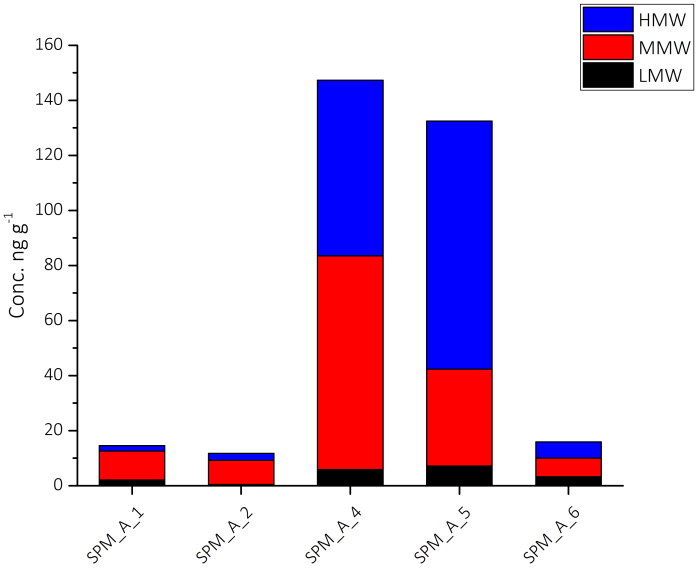

Figure 6.3: LMW, MMW and HMW of PAHs in SPM_A samples.

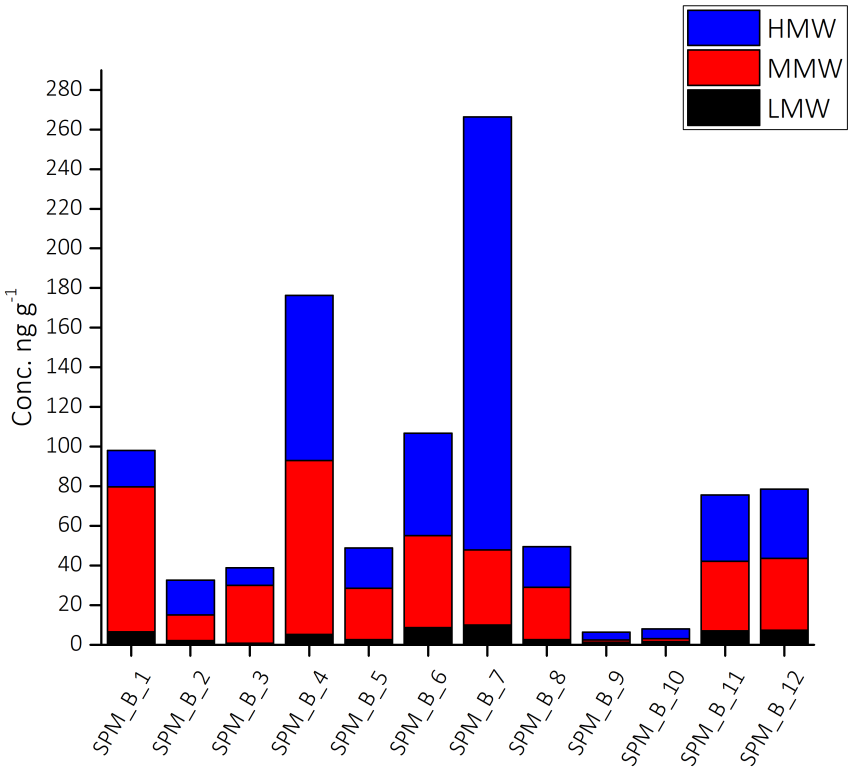

Figure 6.4: LMW, MMW and HMW of PAHs in SPM_B samples.

6.1.3 *n*-Alkanes

The concentrations of single *n*-alkanes were elaborated in the form of indices that are diagnostic for the sources and processes involved in their accumulation in sediments. As reported in paragraph 4.2, the *n*-alkanes are investigated in order to reconstruct the composition of vegetation [66,68]. In particular, the index employed in this thesis is the average chain length (ACL). ACL accounts for the dominant carbon chain in the alkane distribution:

$$ACL = \frac{\sum_{n=21}^{35} (C_n \, x \, n)}{\sum C_n}$$

The short chains (SHC) and long chains (LHC) are calculated in order to determine the predominance between the two and, also, odd and even carbon chains are calculated in order to determine the prevalence between them.

Plants mainly synthesize alkanes with a marked predominance of odd carbon chains, resulting in a typical distribution. In particular, long carbon chains (C_{31}) are representative of herbaceous plants, while short carbon chains (below C_{20}) mainly result from bacterial and algal activity. Chains between C_{20} and C_{29} are representative of plants, in particular C_{27}-C_{29} of terrestrial plants, while C_{21}-C_{25} result from aquatic plants [66,77]. Through the study of the ACL it is also possible to infer climatic changes, since changes in the distribution of carbon chains can reflect variations in the species composition and response of single plants to colder/warmer or drier/wetter conditions [77,78]. Figure shows the result of ACL, odd and even carbon chains and length predominance for SPM_A and SPM_B. In table 6.2 the results of ACL, LHC, SHC, even and odd carbon chains. While in figures 6.5,6.6,6.7 the results of SPM_A samples and in figures 6.8,6.9,6.10 the results of SPM_B samples.

Table 6.2: The results of SPM_A and SPM_B samples.

		ACL	LHS	SHC	EVEN	ODD
SPM_A	Minimum value	28	270	42	165	147
	Maximum value	31	5899	1125	4934	1539
	Number of samples	6	6	6	6	6
	Average value	29	4048	574	3633	984
	Standard deviation	30	2273	384	2046	477
	Coefficient of variation (%)	103%	56%	67%	56%	48%
SPM_B	Minimum value	28	581	15	11	185
	Maximum value	227	12933	2136	7901	8358
	Number of samples	12	12	12	12	12
	Average value	27.9	4545	738	2826	2450
	Standard deviation	0.7	4996	845	3194	3030
	Coefficient of variation (%)	2.5%	109%	114%	113%	123%

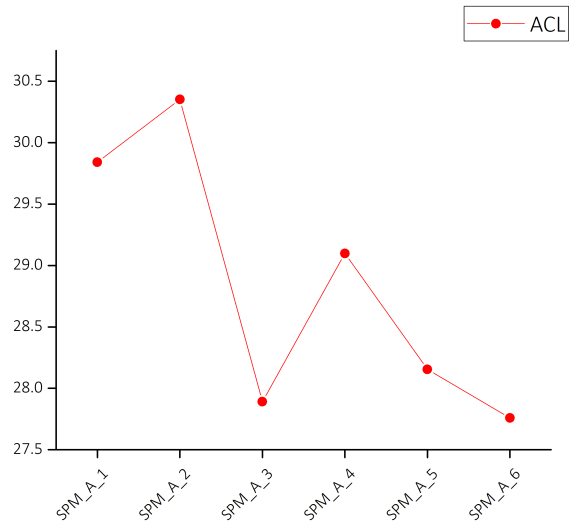

Figure 6.5: ACL index for SPM_A profile.

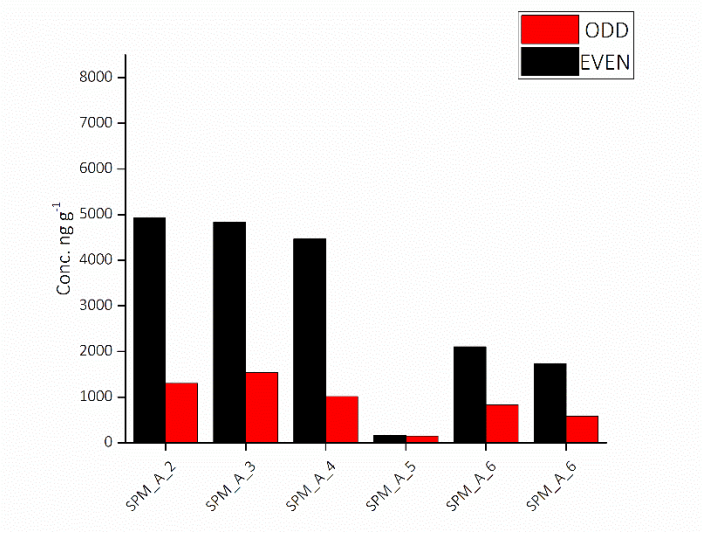

Figure 6.6: odd and even carbon chains of SPM_A profile.

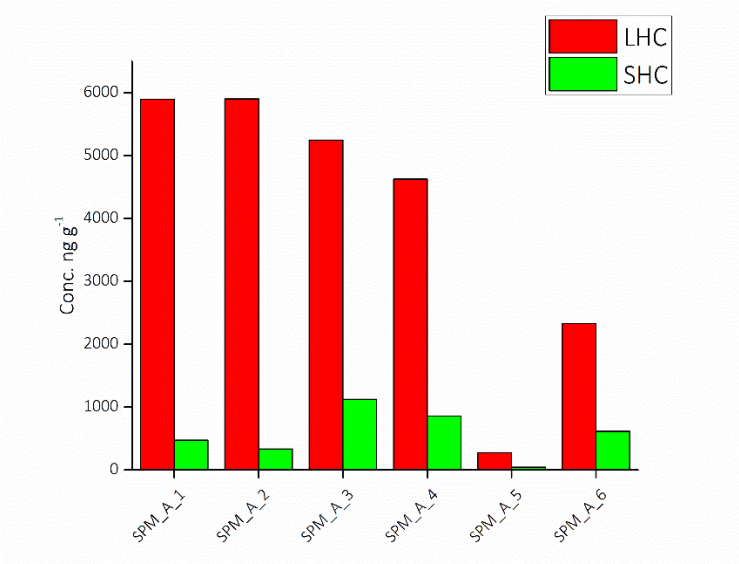

Figure 6.7: LHC and SHC for SPM_A profile.

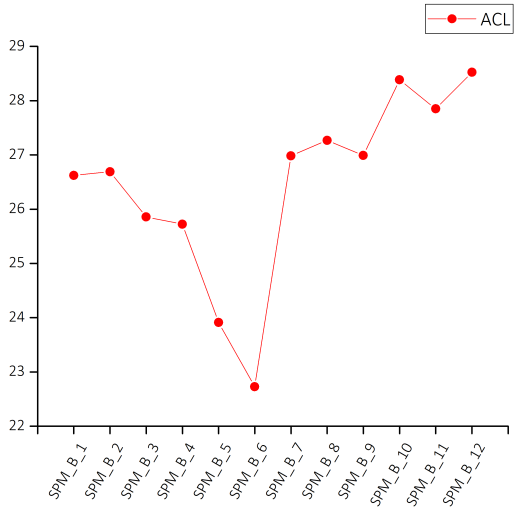

Figure 6.8: ACL index for SPM_B samples.

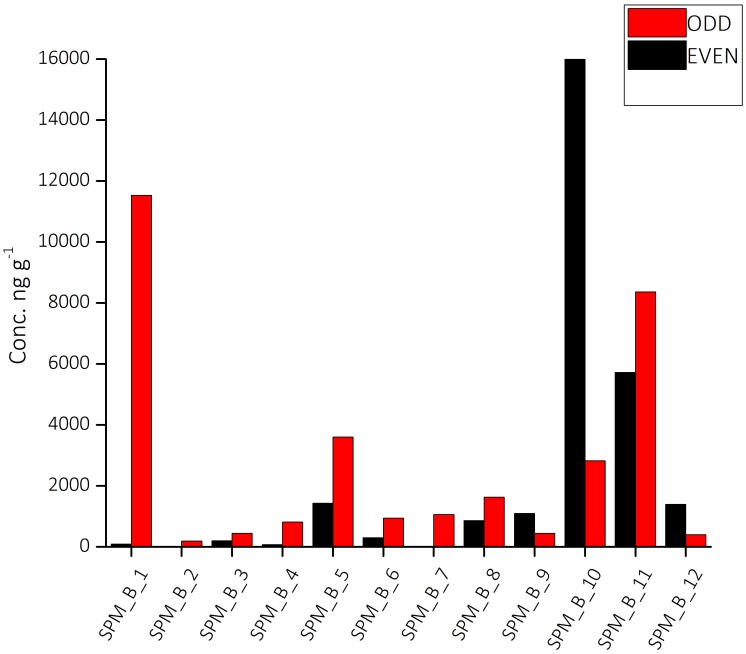

Figure 6.9: odd and even carbon chains from SPM_B samples.

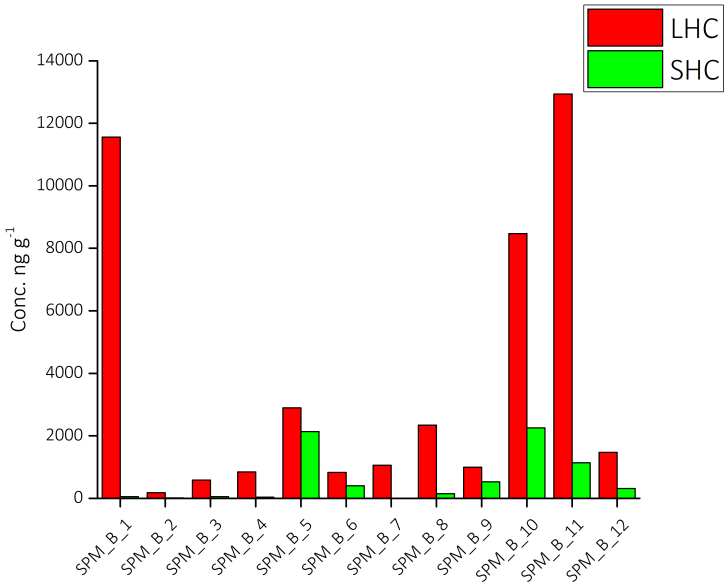

Figure 6.10: LHC and SHC from SPM_B samples.

6.1.4 Charcoal analysis

The charcoal analysis is a study of the concentration and size distribution of charcoal fragments in the samples, which result from the incomplete combustion of biomass. Results are shown in fig. 6.11 as concentrations (pieces per gram of dry sample) divided by five dimensional classes.

The sum of SPM_A results of charcoal analysis has a range between 11 and 49 counts g^{-1}.

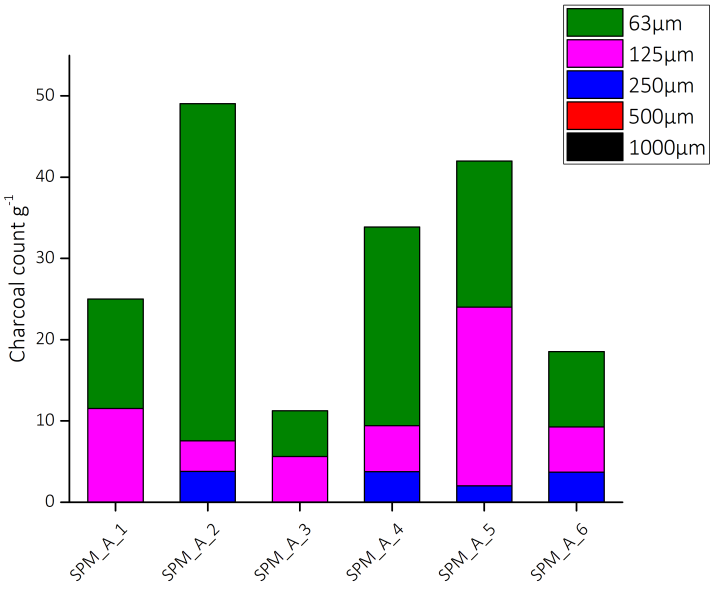

Figure 6.11: Charcoal distribution in SPM_A samples.

The sum of SPM_B results (*fig. 6.12*) of charcoal analysis has a range between 16 and 47 counts g^{-1}.

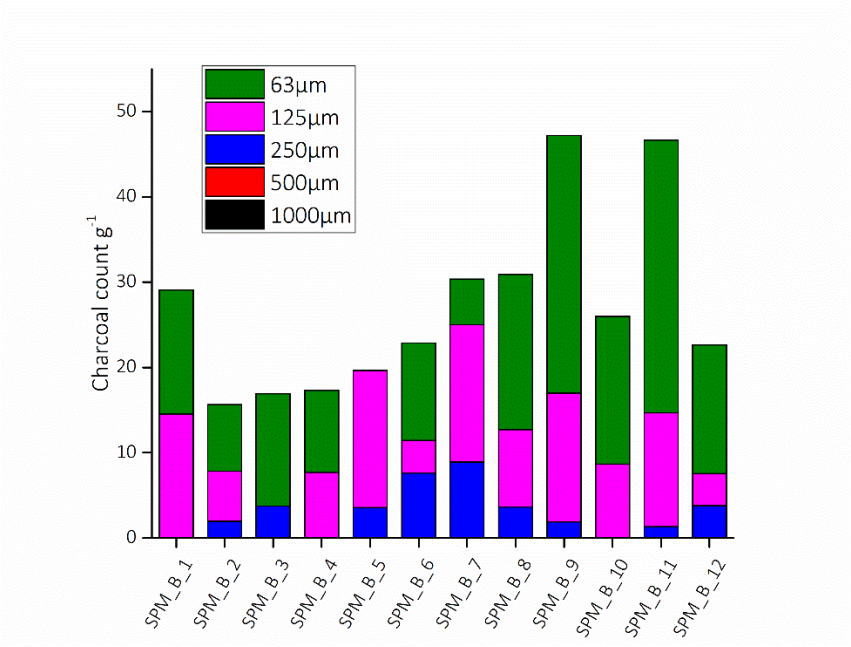

Figure 6.12: Charcoal distribution in SPM_B samples.

6.1.5 Anhydrous monosaccharides (AMs)

The AMs are specific tracers of biomass burning, in particular the levoglucosan is the main product of the thermal degradation of cellulose [57]. Mannosan and galactosan are two isomers of

levoglucosan, the isomers are subjected to the temperature of the fire and are produced by the combustion of hemicelluloses.

Concentrations of levoglucosan, mannosan and galactosan (ng g^{-1}) for SPM_A and SPM_B are summarized in table 6.3. in figures 6.13 and 6.14 the results from both sampling sites.

Table 6.3: Anhydrous monosaccharides concentrations in SPM_A and SPM_B, given as maximum, minimum and average concentrations

		Levoglucosan	Mannosan	Galactosan
SPM_A (ng g^{-1})	Minimum value	14	0.4	1
	Maximum value	84.7	07	6.6
	Number of samples	6	6	6
	Average value	43	0.7	3
	Standard deviation	25	0.3	2
	Coefficient of variation (%)	50%	42%	67%
SPM_B (ng g^{-1})	Minimum value	10.4	0.3	2.2
	Maximum value	143.4	9.7	17.2
	Number of samples	12	12	12
	Average value	116.4	2.9	5.7
	Standard deviation	24.2	3.4	5.5
	Coefficient of variation (%)	20%	113%	96%

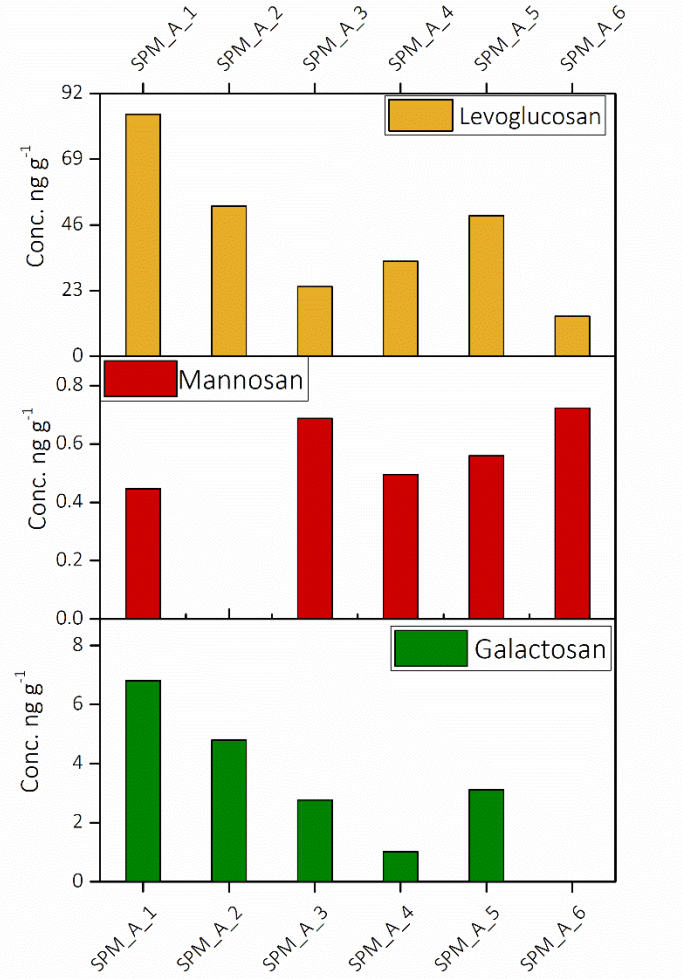

Figure 6.13: Anhydrous monosaccharides content in SPM_A samples.

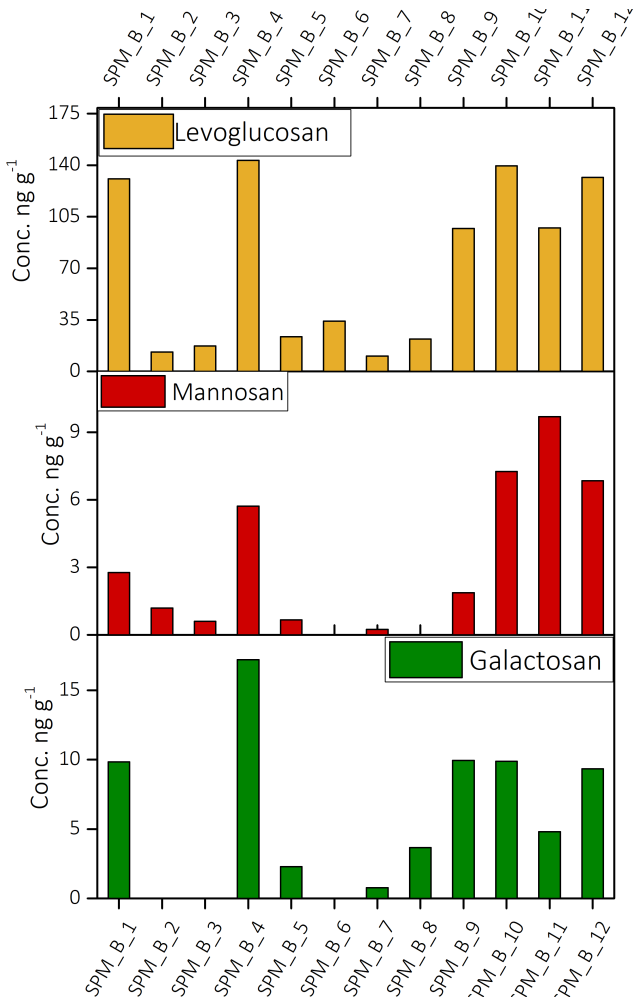

Figure 6.14: Anhydrous monosaccharides content in SPM_B samples.

6.1.6 Miliacin

The miliacin molecule is the characteristic component of broomcorn millet (*Panicum miliaceum)*. Since this species was cultivated, the presence of miliacin is diagnostic for human presence [45]. Table 6.4 shows the results from SPM_A and SPM_B samples. The graphs are showed in figure 6.15 and 6.16

Table 6.4: miliacin concentration from SPM_A and SPM_B samples.

	SPM_A (ng g^{-1})	SPM_B (ng g^{-1})
Minimum values	95.3	80.4
Maximum values	268.3	313.3
Average values	189	273
Standard deviation	62	75

Coefficient of variation (%)	33%	43%

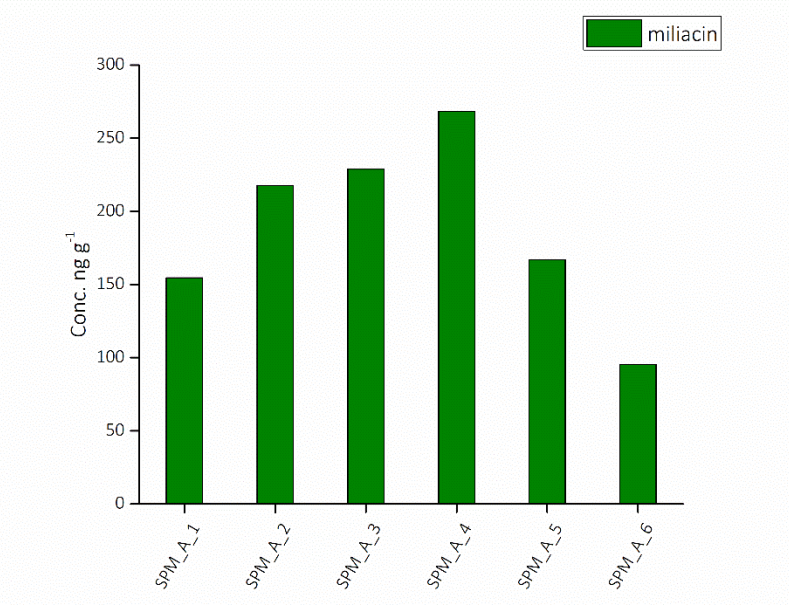

Figure 6.15: Miliacin concentrations in SPM_A samples.

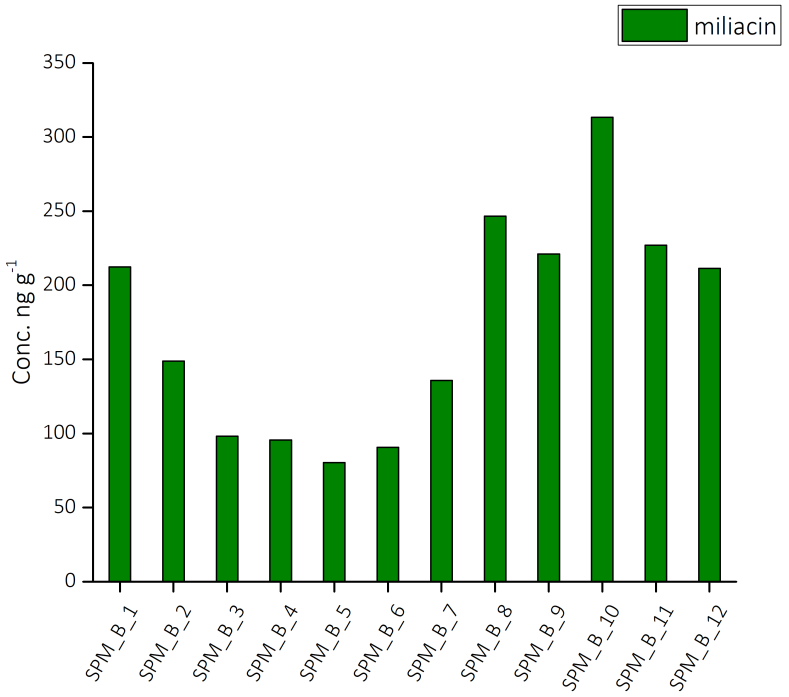

Figure 6.16: Miliacin concentrations in SPM_B samples.

6.1.7 Fecal, plants and fungal sterols (FPFS)

Fecal sterols are generally investigated as tracers of fecal contamination in wastewater and soil. In the case of the DE, it is known that the soil was strongly affected by human activities. To better reconstruct the human presence in the samples two indices were employed [79]. In particular, the indices used are:

$$Human\ contribution\ (HC) = \frac{(Coprostanol + Epi\text{-}coprostanol)}{(Cholesterol + Cholestanol)}$$

$$Vegetal\ contribution\ (VC) = \frac{\beta\text{-}Sitosterol}{Stigmastanol}$$

Table 6.5 shows the results for sterols from the SPM_A and SPM_B sampling profiles. The figures 6.17 and 6.18 present the result for FPFS.

Table 6.5: results of sterols from SPM_A and SPM_B, reported as minimum, maximum and average values.

		Human contribution	Vegetal contribution
SPM_A	Minimum value	0.68	0.65
	Maximum value	0.83	1.72
	Number of samples	6	6
	Average value	0.7	0.9
	Standard deviation	0.1	0.4
	Coefficient of variation (%)	14%	44%
SPM_B	Minimum value	0.61	0.26
	Maximum value	1.13	0.96
	Number of samples	12	12
	Average value	0.8	0.6
	Standard deviation	0.2	0.1
	Coefficient of variation (%)	26%	16%

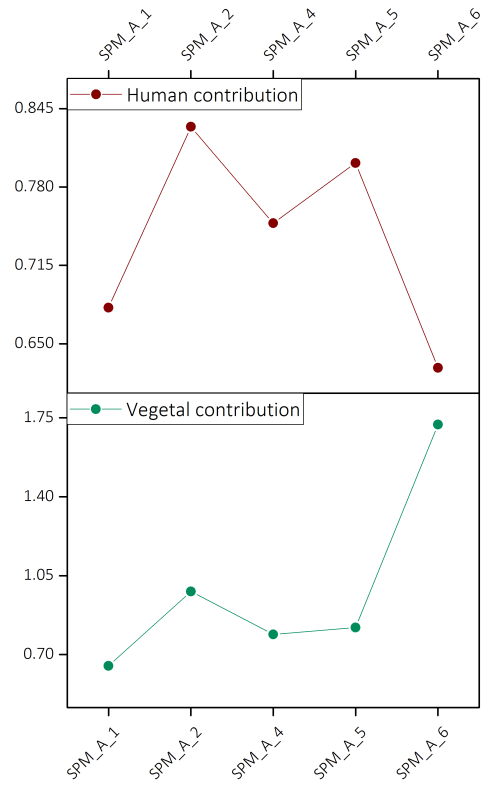

Figure 6.17: Variation of human and vegetal contributions in SPM_A samples.

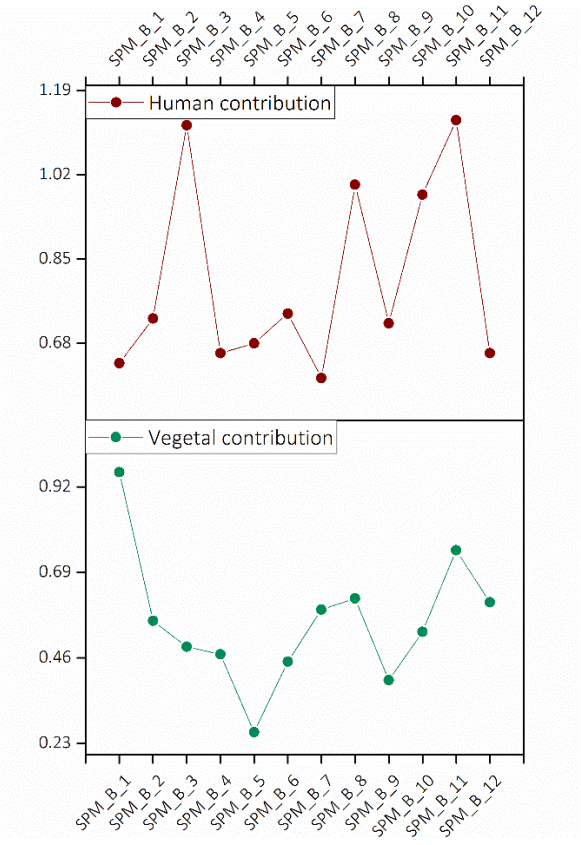

Figure 6.18: Human and vegetal contributions in SPM_B samples.

6.2 Verona: Via Pigna (VP)

6.2.1 Total and organic carbon

The total and organic carbon are present as amount per cent, for the two-sampling site VP_A and VP_B.

The total carbon for the VP_A has a range between 3.8 % and 10.3 %, the average value is 8.2 % ± 3.1 %. The organic carbon for the same sampling site has a range between 2.4 % and 7.9 %, the average value is 6.4 % ± 2.2 %. Figure 6.19 represents the percent amount of total and organic carbon.

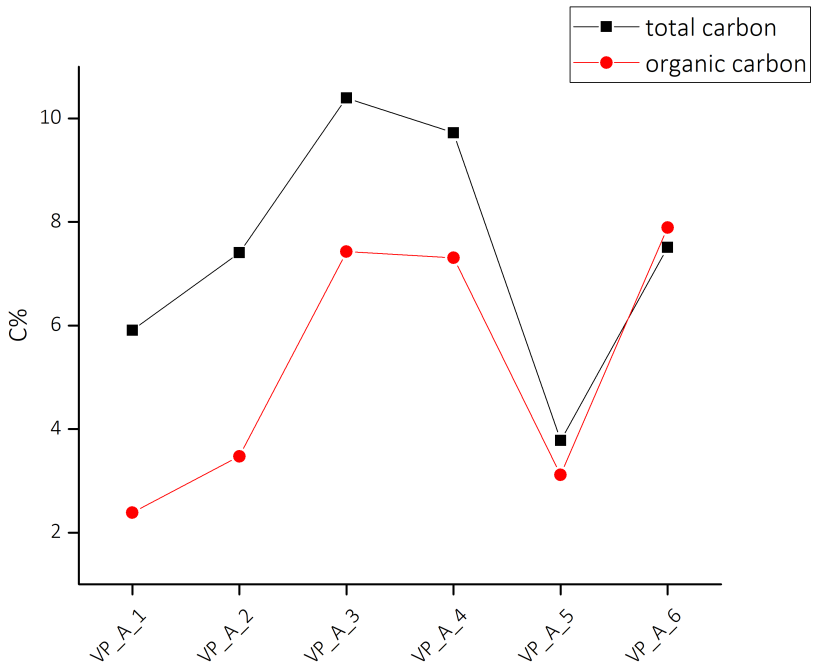

Figure 6.19: Graph of content of total and organic carbon in VP_A samples.

The total carbon for the VP_B has a range between 3.5 % and 9.5 %, the average values is 6.1 % ± 3.9 %. The organic carbon for the same sampling site has a range between 2.1 % and 8.1 %, the average values is 4.4 % ± 2.5 %. Figure 6.20 represents the percent amount of the total and organic carbon.

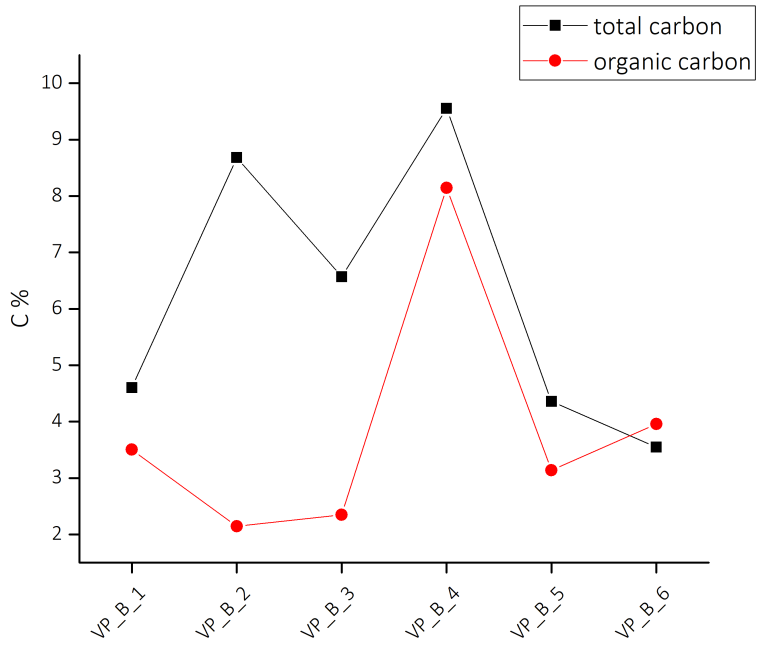

Figure 6.20: content of total and organic carbon in VP_B samples.

6.2.2 Polycyclic Aromatics Hydrocarbons (PAHs)

The sum of PAHs are presented as LMW, MMW and HMW for both profile sampling site VP_A and VP_B. In the table 6.6 are presented the range and the mean values for each sampling sites.

Table 6.6: results of PAHs from VP_A and VP_B.

		LMW	MMW	HMW
VP_A (ng g^{-1})	Minimum value	0.4	3.56	2.7
	Maximum value	5.7	20.7	71.4
	Number of samples	6	6	6
	Average value	1.7	10.8	29.2
	Standard deviation	1.8	6.2	28.3
	Coefficient of variation (%)	106%	57%	98%
VP_B (ng g^{-1})	Minimum value	0.6	3	1
	Maximum value	11.6	128.6	110.8
	Number of samples	12	12	12
	Average value	3.3	22.2	22.4

	Standard deviation	3.9	38.9	33.3
	Coefficient of variation (%)	118%	175%	148%

Figures 6.21 and 6.22 represent the LMW, MMW and HMW concentrations of PAHs detected in the sample from VP_A and VP_B, as reported table6.6.

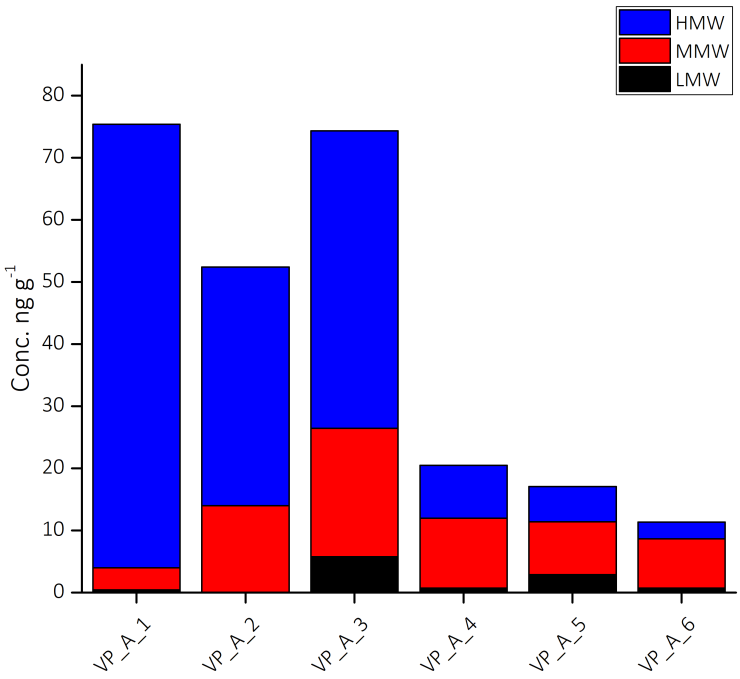

Figure 6.21: LMW, MMW and HMW of PAHs in VP_A samples.

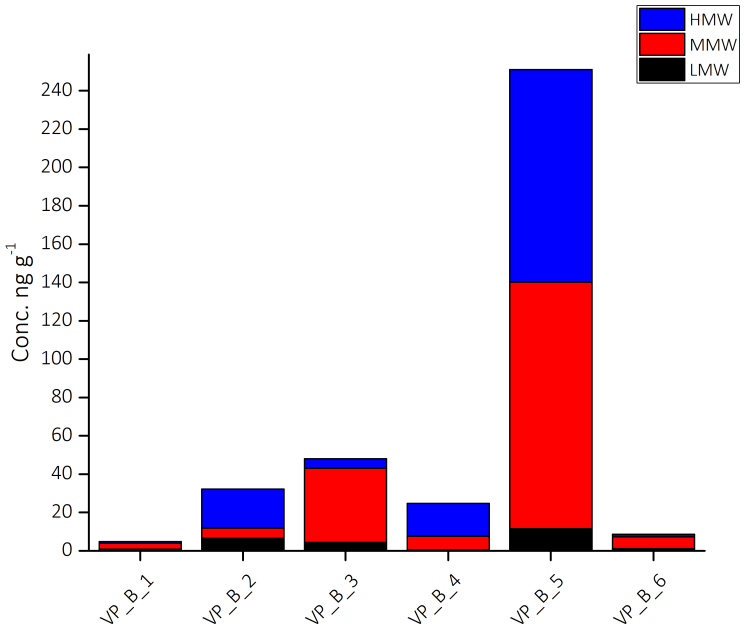

Figure 6.22: LMW, MMW and HMW of PAHs in VP_B samples.

6.2.3 *n*-Alkanes

The results of n-alkanes are presented with the ACL index, and the comparison between LHC, SHC, odd and even chains for both sites VP_A and VP_B (tab. 6.7).

Table 6.7: n-Alkanes results from VP_A and VP_B samples.

		ACL	LHC	SHC	EVEN	ODD
VP_A	Minimum value	22	62	77	32	127
	Maximum value	30	5918	637	5576	1113
	Number of samples	6	6	6	6	6
	Average value	26.1	1787	332	1673	497
	Standard deviation	3.7	2336	222	2157	377
	Coefficient of variation (%)	14%	130%	66%	128%	75%
VP_B	Minimum value	22	86	11	9	86
	Maximum value	28	5129	5792	10108	4283
	Number of samples	6	6	6	6	6
	Average value	25.1	3791	1469	3733	1748
	Standard deviation	2.3	4682	4336	4336	1811
	Coefficient of variation (%)	9%	123%	295%	116%	103%

In the figures 6.23, 6.24, 6.25, 6.26, 6.27, 6.28 ACL indexes, comparisons between LHC and SHC chains, and comparisons between even and odd chains from VP_A and VP_B profiles are represented.

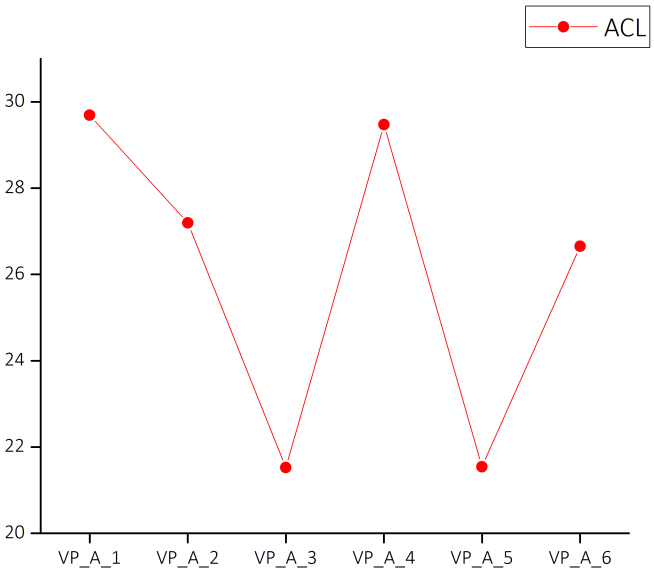

Figure 6.23: ACL index for VP_A samples.

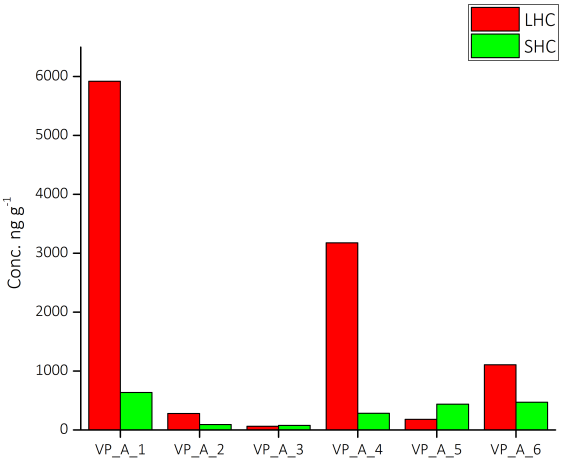

Figure 6.24: LHC and SHC from VP_A samples.

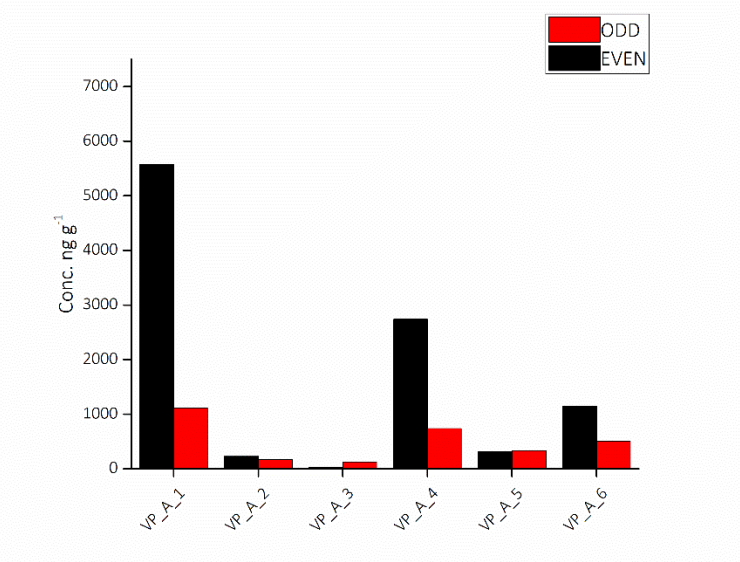

Figure 6.25: odd and even chains from VP_A.

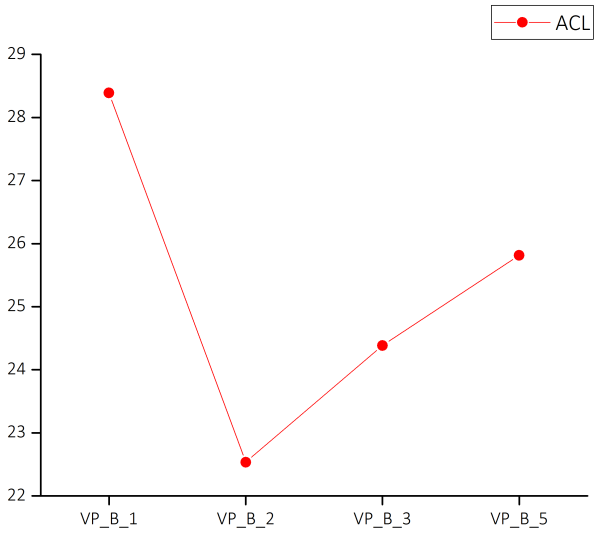

Figure 6.26: ACL index for VP_B samples.

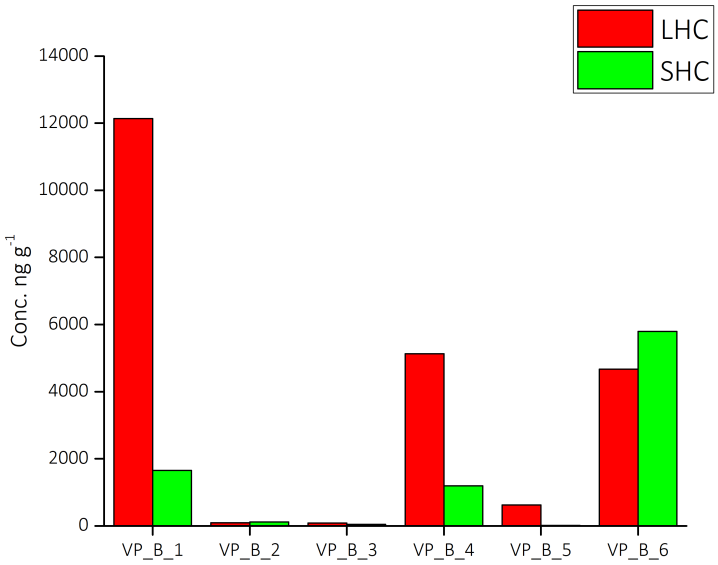

Figure 6.27:LHC and SHC from VP_B samples.

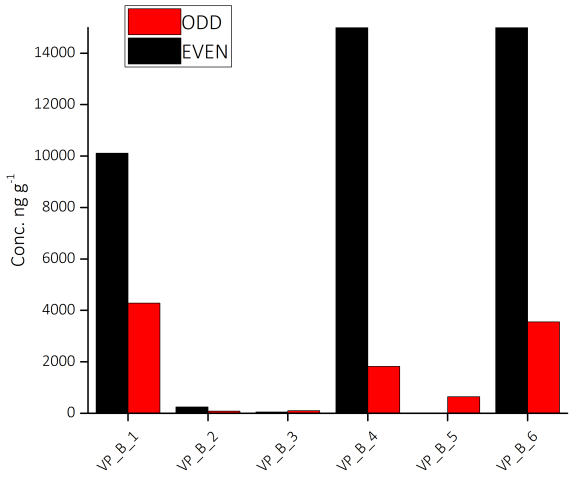

Figure 6.28: odd and even chains from VP_B samples.

6.2.4 Charcoal analysis

The sum of VP_A results from the charcoal analysis ranges between 25 and 274 counts g^{-1}, with the average value of 153± 129. Figure 6.29 shows the results of charcoal analysis.

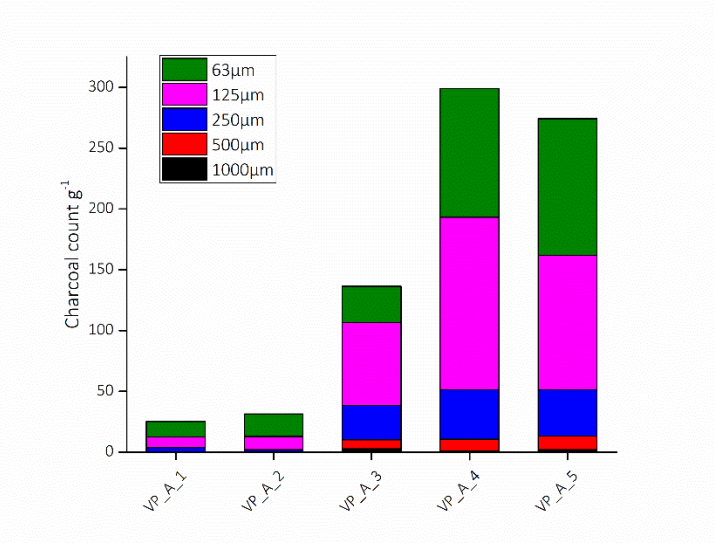

Figure 6.29: Charcoal distribution in VP_A samples.

The sum of VP_B results of charcoal analysis has a range between 45 and 180 counts g^{-1}, with the average value of 129 ± 83 pieces g^{-1} (in fig. 6.30)

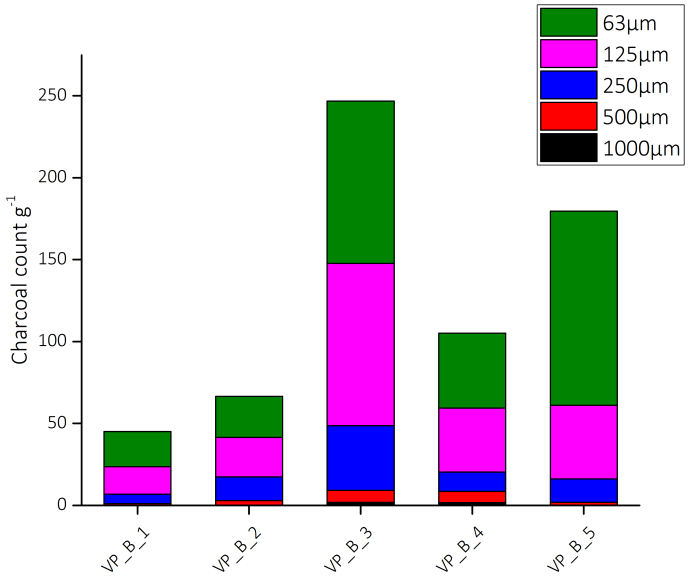

Figure 6.30: Charcoal distribution in VP_B samples.

6.2.5 Anhydrous monosaccharides (AMs)

The results from the two sampling profiles (VP_A and VP_B) are presented as the concentration of the levoglucosan, mannosan and galactosan in table 6.8. Figures 6.31 and 6.32 the results.

Table 6.8: maximum, minimum and average value from VP_A and VP_B sampling sites.

		LMW	MMW	HMW
VP_A (ng g^{-1})	Minimum value	0.4	3.6	2.7
	Maximum value	5.7	20.7	71.4
	Number of samples	6	6	6
	Average value	1.7	10.9	29.1
	Standard deviation	2.2	5.9	27.9
	Coefficient of variation (%)	129%	53%	96%
VP_B (ng g^{-1})	Minimum value	0.6	3	1
	Maximum value	11.6	128.7	110.8
	Number of samples	12	12	12
	Average value	3.5	21.7	22.4
	Standard deviation	3.7	38.9	33.3
	Coefficient of variation (%)	106%	179%	149%

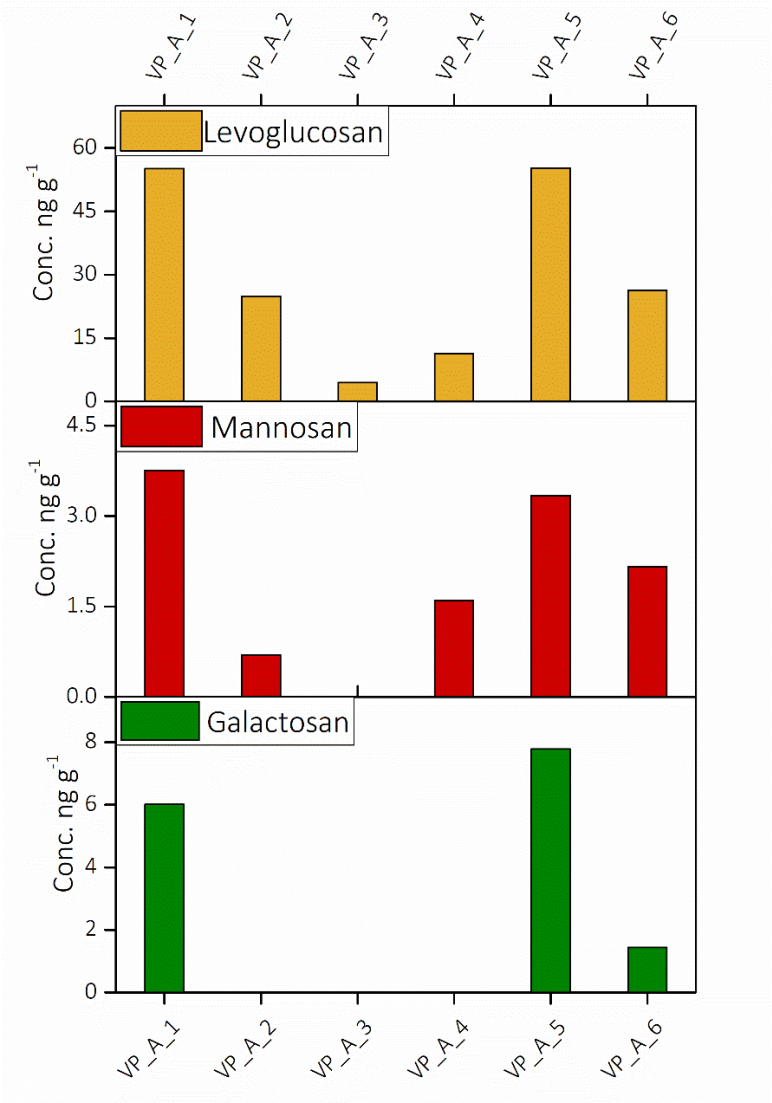

Figure 6.31: concentrations of levoglucosan, mannosan and galactosan in VP_A samples.

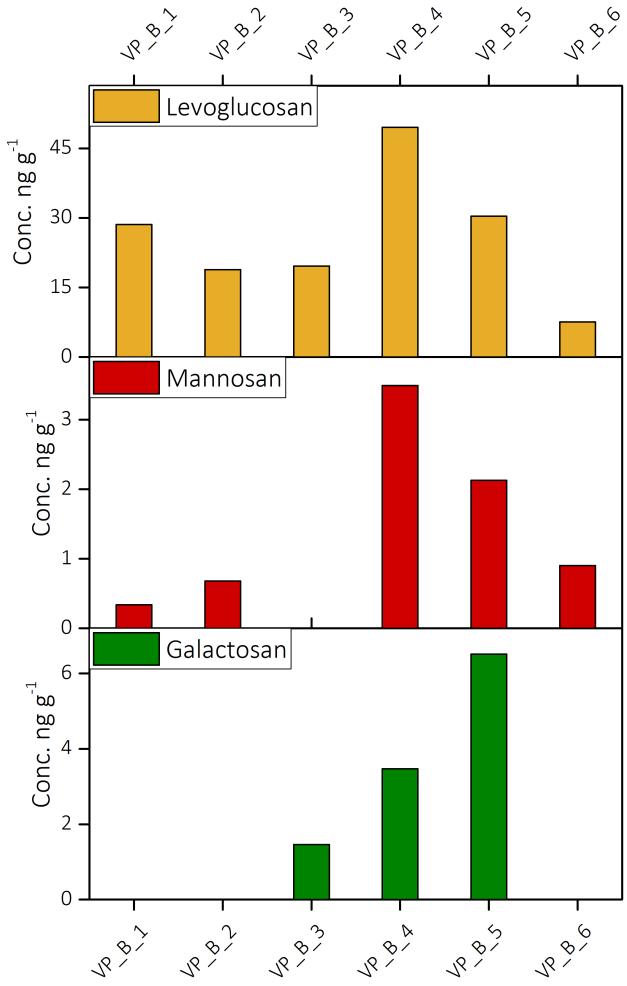

Figure 6.32: concentrations of levoglucosan, mannosan and galactosan from VP_B samples.

6.2.6 Miliacin

The results are presented as concentration of miliacin (ng g^{-1}), for both sampling sites (VP_A and VP_B) (*tab.6.9*).

Table 6.9: concentrations of miliacin in VP_A and VP_B samples.

	VP_A (ng g^{-1})	VP_B (ng g^{-1})
Minimum values	116.4	3.5
Maximum values	316.2	274.6
Average values	124.4	97.1
Standard deviation	13.1	104.3
Coefficient of variation (%)	10%	107%

Figures 1.33 and 1.34 represents the miliacin concentration detected in VP_A and VP_B profiles.

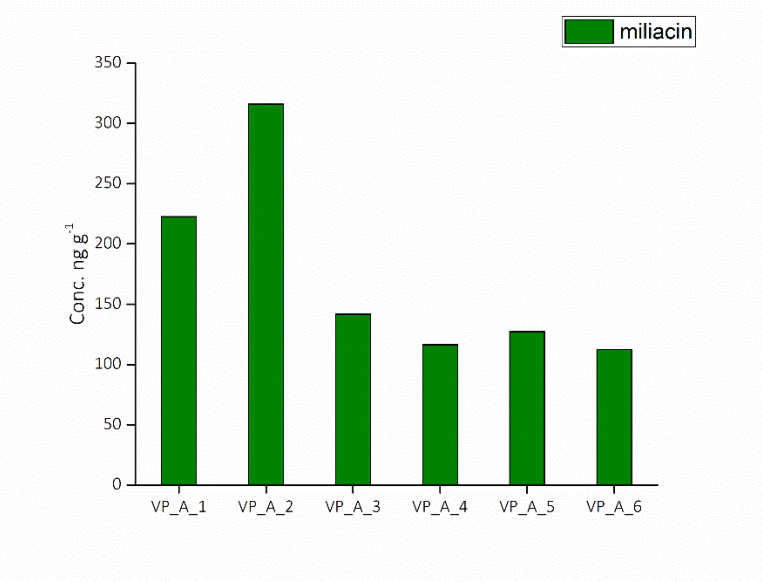

Figure 6.33: Miliacin concentration detected in VP_A samples.

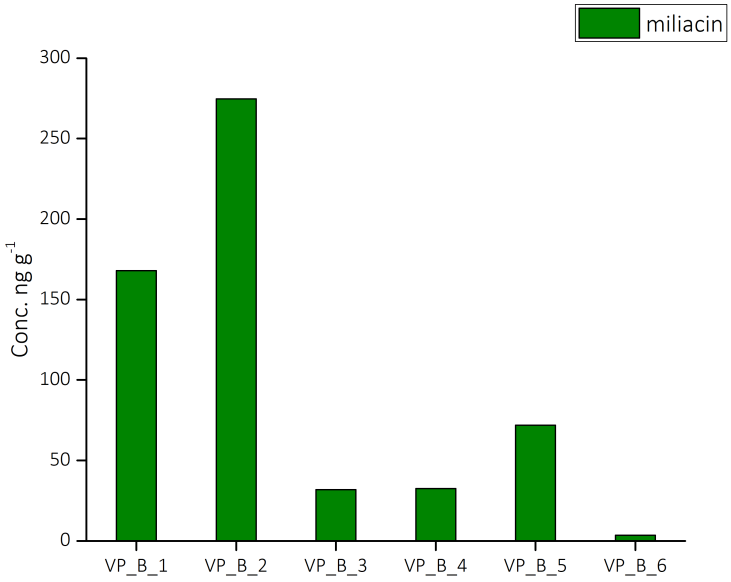

Figure 6.34: Miliacin concentration detected in VP_B samples.

6.2.7 Fecal, plants and fungal sterols (FPFS)

Fecal, plants and fungal sterols concentrations from VP_A and VP_B profiles are represented in the table 6.10 and in the figures 6.35 and 6.36.

Table 6.10: results of sterols from VP_A and VP_B.

		Human contribution	Vegetal contribution
VP_A	Minimum value	0.5	0.3
	Maximum value	1.4	0.9
	Number of samples	6	6
	Average value	1.1	0.6
	Standard deviation	0.4	0.2
	Coefficient of variation (%)	36%	33%
VP_B	Minimum value	0.6	0.7
	Maximum value	1.3	1.7
	Number of samples	12	12
	Average value	0.8	0.9
	Standard deviation	0.4	0.2
	Coefficient of variation (%)	50%	22%

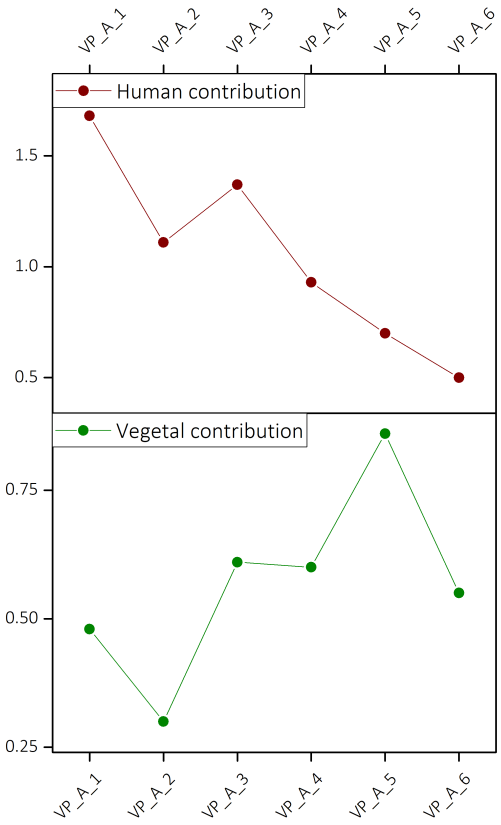

Figure 6.35: Human and vegetal contributions of VP_A samples.

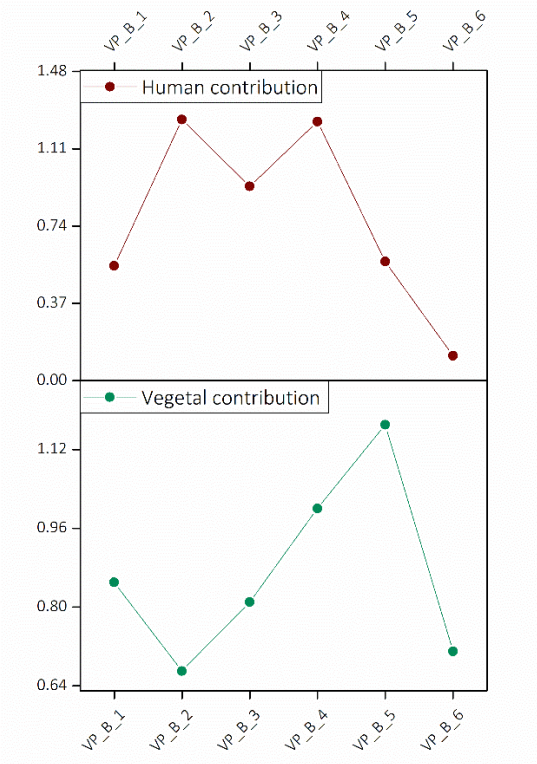

Figure 6.36: Human and vegetal contributions of VP_B samples.

6.3 Belluno: Mel (MEL)

6.3.1 Total and organic carbon

The total and organic carbon are presented as amount per cent, for the sampling site MEL.

The total carbon for MEL samples ranges between 4.2 % and 6.5 %, the average value is 5.8 % ± 0.8 %. The organic carbon for the same sampling site has a range between 3.1 % and 6.4 %, the average values is 4.3 % ± 1.5 %. Figure 6.37 represents the per cent amount of total and organic carbon.

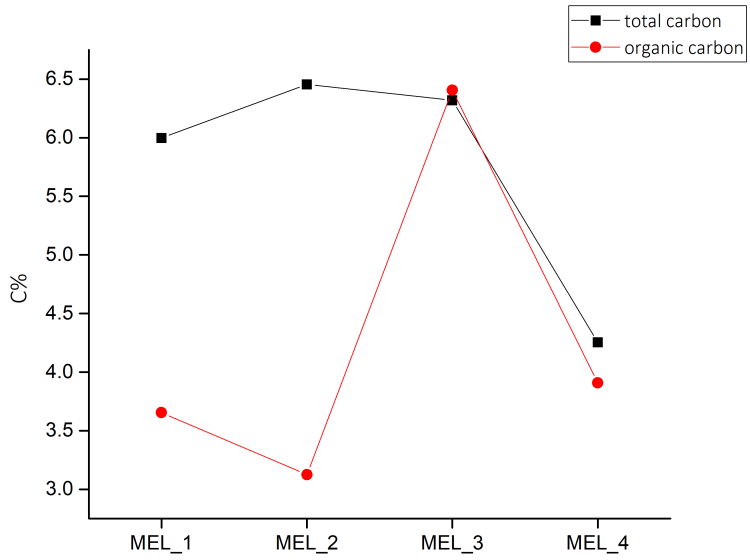

Figure 6.37: Graph of total and organic carbon content in MEL samples.

6.3.2 Polycyclic Aromatics Hydrocarbons (PAHs)

PAH concentrations are presented as sum of LMW, MMW and HMW for sampling site. In the table 6.11 are presented the minimum, maximum and mean values from the sampling site. Figure 6.38 shows the results from each sample.

Table 6.11: PAHs from MEL.

		LMW	MMW	HMW
	Minimum value	1.2	1.1	4
	Maximum value	6	12.2	19.1

MEL (ng g^{-1})	Number of samples	4	4	4
	Average value	2.8	7	11.7
	Standard deviation	2.3	5.4	6.4
	Coefficient of variation (%)	82%	77%	54%

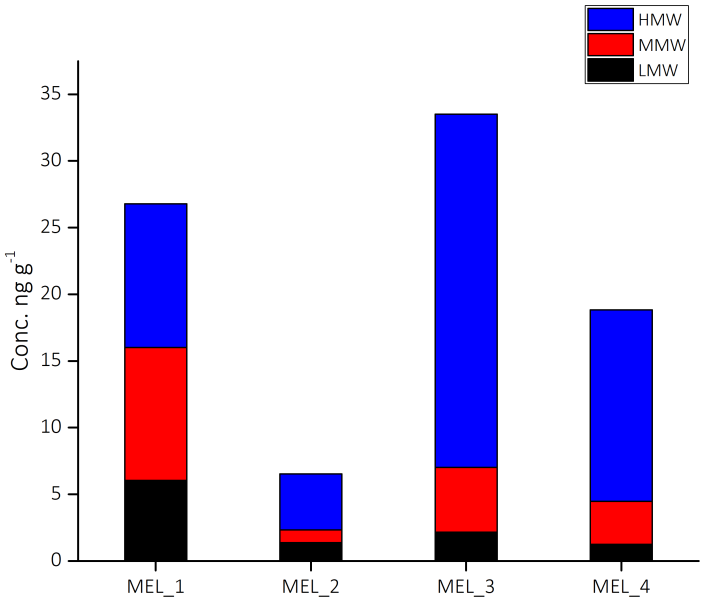

Figure 6.38: LMW, MMW and HMW of PAHs from MEL samples.

6.3.3 *n*-Alkanes

The *n*-alkanes for the samples from MEL are presented here using the same parameters introduced above. Table 6.12 shows the values of ACL index, LHC and SHC, odd and even chain concentrations.

Table 6.12: n-Alkanes parameters for MEL samples.

		ACL	LHC	SHC	even	odd
MEL	Minimum value	21.9	86	95	93	87
	Maximum value	31.56	4842	498	4576	765
	Number of samples	4	4	4	4	4
	Average value	28.3	2398	228	2285	341
	Standard deviation	4.3	2240	224	2107	299

	Coefficient of variation (%)	15%	93%	98%	92%	87%

Figures 6.39, 6.40 and 6.41 show the parameters for each sample coming from MEL profile.

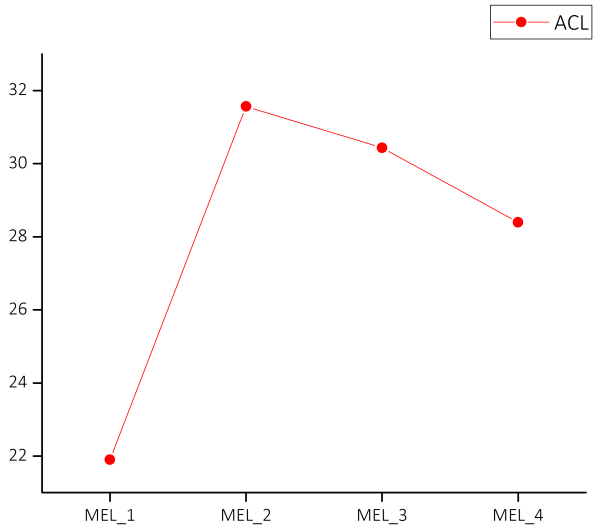

Figure 6.39: Graph of ACL index detected in MEL samples.

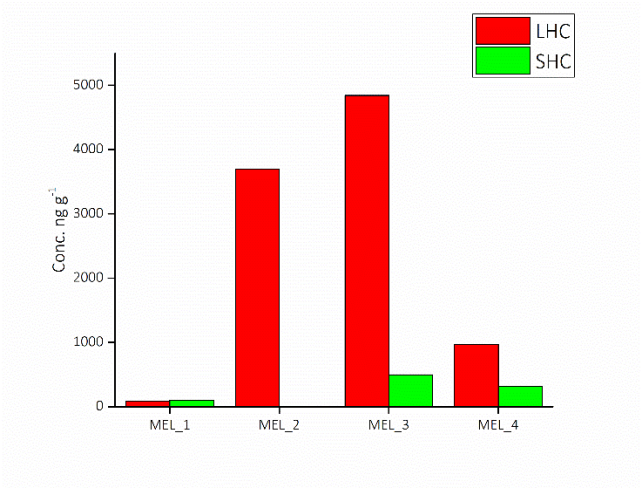

Figure 6.40: LHC and SHC of MEL samples.

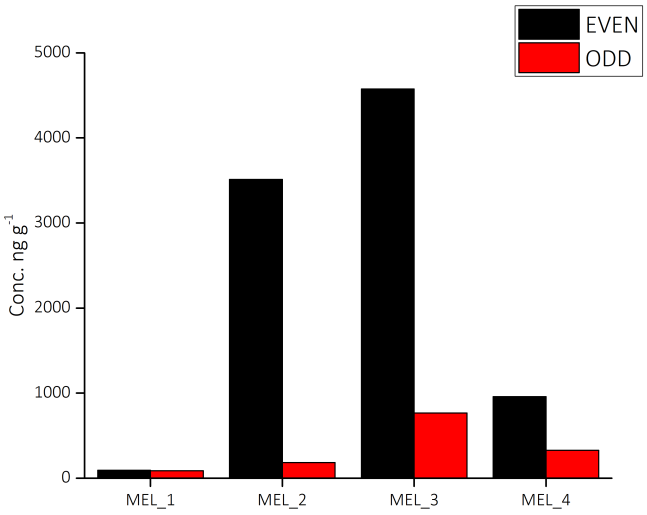

Figure 6.41: odd and even chains from MEL samples.

6.3.4 Charcoal analysis

The sum of MEL results from charcoal analysis ranges between 10 and 25 counts g^{-1} with the average value of 18±7 counts g^{-1} (*fig. 6.42*).

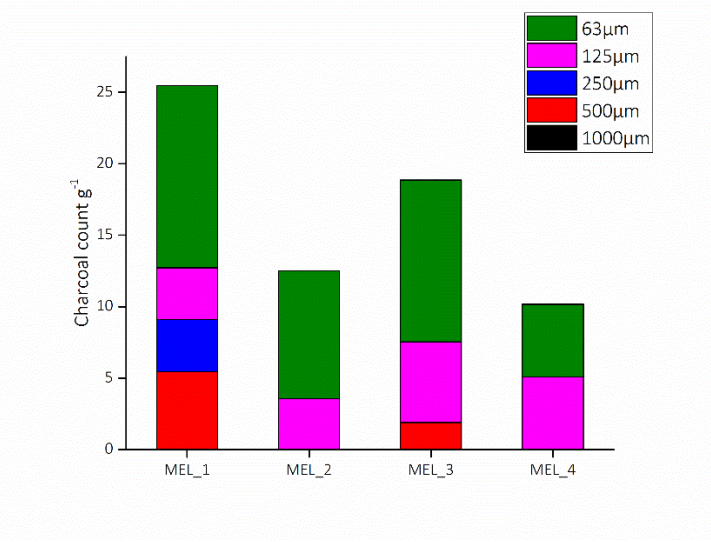

Figure 6.42: Charcoal distribution in MEL samples.

6.3.5 Anhydrous monosaccharides (AMs)

Table 6.13 shows the levoglucosan, mannosan and galactosan concentrations quantified in the MEL samples (*fig. 6.43*)

Table 6.13: MAs values from MEL samples.

		Levoglucosan	Mannosan	Galactosan
MEL (ng g^{-1})	Minimum value	6	nd	nd
	Maximum value	1.2	nd	nd
	Number of samples	4	4	4
	Average value	2.7	nd	nd
	Standard deviation	2.3	nd	nd
	Coefficient of variation (%)	85%	nd	nd

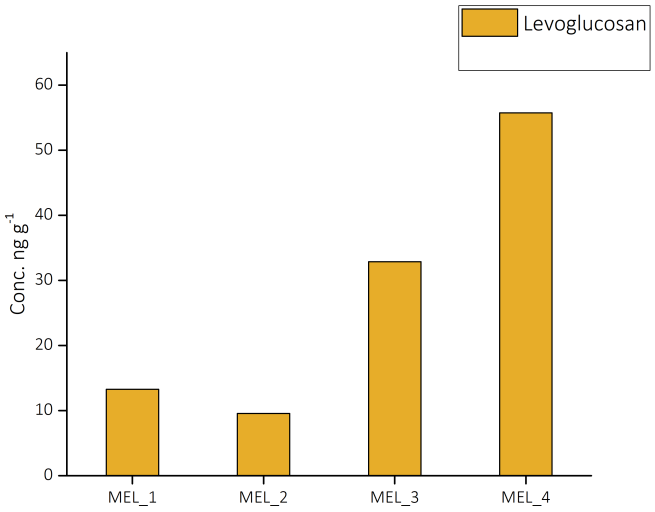

Figure 6.43: Concentration of levoglucosan in MEL samples.

6.3.6 Miliacin

Table 6.14 and figure 6.44 display the concentrations (ng g^{-1}) of miliacin from the MEL samples.

Table 6.14: miliacin concentration from MEL samples.

	MEL (ng g^{-1})
Minimum value	171.6
Maximum value	480.9
Average value	250.4
Standard deviation	157.3

Coefficient of variation (%)	63%

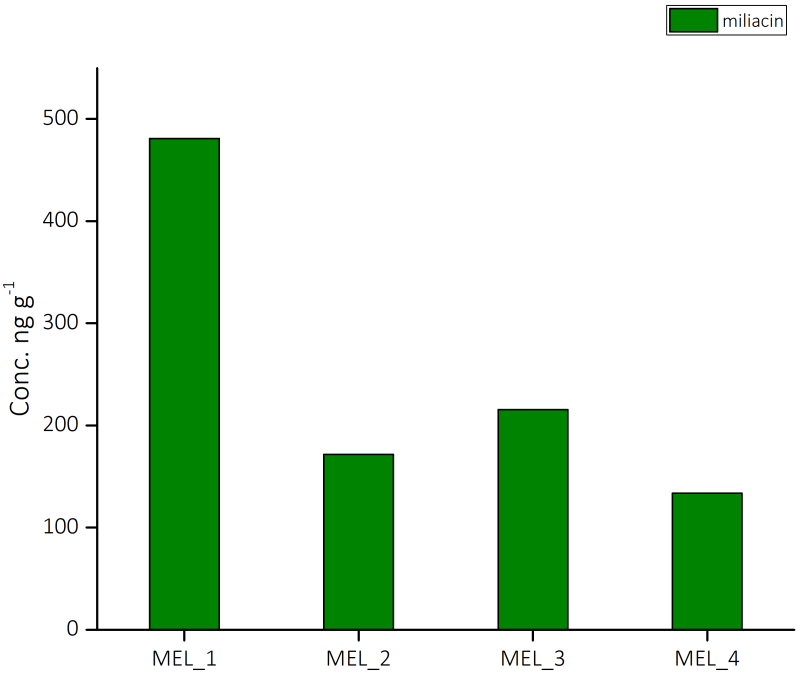

Figure 6.44: Miliacin concentration detected in MEL samples.

6.3.7 Fecal, plants and fungal sterols (FPFS)

In the table 6.15 are presented the sterol results obtained from the MEL sampling site.

Table 6.15: Sterols from MEL samples.

		Human contribution	Vegetal contribution
MEL	Minimum value	0.12	0.62
	Maximum value	1.03	1.84
	Number of samples	4	4
	Average value	0.7	1.3
	Standard deviation	0.4	0.6
	Coefficient of variation (%)	57%	46%

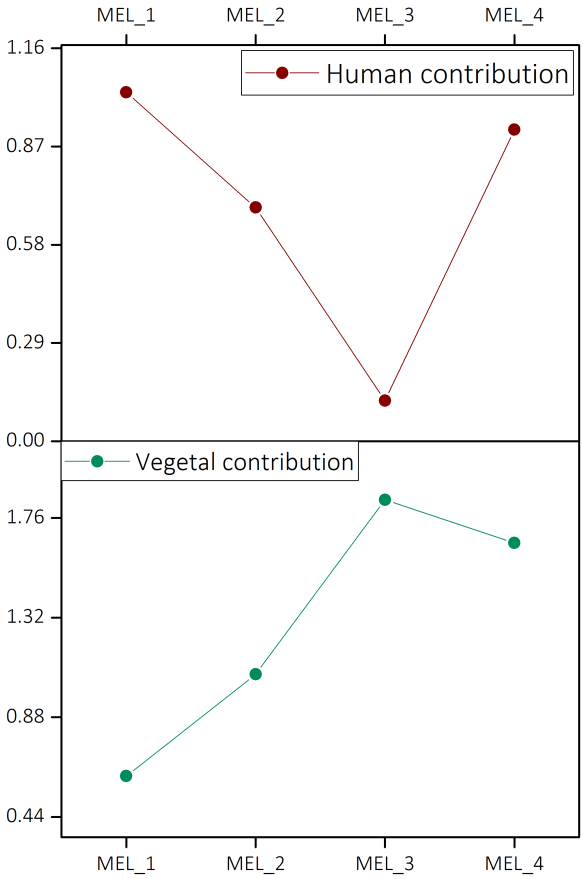

Figure 6.45: Human and vegetal contribution in MEL samples.

7 DISCUSSION

The discussion will be based on the archeological site area: Verona-SPM, Verona-VP and Belluno-MEL. The results show a strong inter-site and inter-sample variability. This is probably related to the fact that the soil underwent strong reworking and is strongly influenced by human activities, so the interpretation was not straightforward.

7.1 Verona: Vicolo San Pietro in Monastero (SPM)

The Vicolo San Pietro in Monastero (SPM) site presented a great variability between the samples, likely due to the strong reworking that is characteristic of DE. In this thesis fire events as a result of human activities were investigated: in particular, PAHs and AMs as proxies of fire were detected and interpreted also according to the charcoal distribution. Results suggest that probably fire activities were important in SPM sites. In particular, from the study of AMs it arises that the principal biomass burning source are likely cellulose and hemicellulose, which is coherent with the use of wood as main fuel. However, in some samples of SPM (in particular: SPM_B_6) no mannosan and galactosan were detected, probably because the fire was prolonged in time [64]. Also, the absence of mannosan and galactosan and the relatively low concentration of levoglucosan could result from the natural soil washing away, because these molecules are water soluble. The source of the AMs might be identified in domestic fireplaces, and maybe a little productive activity (e.g. trade, farming, agriculture) because the level of AMs and PAHs are not so high to justify extended fire events, but rather a continuous accumulation of ashes and charred material that was thrown away. Mainly MMW and HMW PAHs were detected, leading to the conclusion that the fire source was close to the deposition site [57,58]. In fact, MMW and HMW PAHs are heavier and tend to accumulate in the neighborhood, so it is possible to affirm that PAHs were originate from the domestic fireplaces. Therefore, the PAHs and AMs give similar information about the use of fire in this area: fire was used on a daily basis and waste was accumulated in these soils.

Another evidence of the presence of fire is charcoal. Charcoal was investigated based on the size distribution, obtained by sifting samples with five decreasing dimensional class sieves and by counting charcoal fragments [48]. From this analysis, it emerges that the number of charcoal pieces increases with the decrease in particle size. For this reason, the origin of the charcoal is likely to be identified in ashes, smooth and charred materials that can be fragmented again and again thanks to the reworking that is characteristic of DE. The soils were strongly undergone to a continuous use, mixing and accumulation on it, so for this reason these soils are reworked. Probably, the charcoal is the main responsible of the dark color of DE [47]. The fraction below 63 µm could not be analyzed, so the information about this dimensional class of potential interest is lost. Moreover, the average value of organic carbon detected in samples (4%), significantly higher than DE typical values (0.5-2%) related only to the organic matter content [47], suggests charcoal as its primary source in the SPM site.

The other proxies that were investigated are fecal and plant fungal sterols (FPFS), that are used to detected human presence in soils. The DE are anthropic soils that underwent strong modifications by humans. Through the FPFS analysis, it is possible to reconstruct the human presence and also the activities that involved the area [74,79]. In particular, the index of human contribution reveals that humans were present continuously and fecal material was accumulated on these soils. Moreover, the plant sterol contribution can suggest also the presence of ruminants, since livestock breeding was likely practiced.

High concentrations of miliacin were found in SPM DE since the inhabitants probably used millet for food purposes. Millet was not subject to taxes, so it was consumed by the poor people, and/or used to feed animals [44,70]. Also, millet is a resistant plant that can be found in many environments such as the valley and hilly zones [43]. The high concentrations of miliacin could result also from another use of the millet stalks: they were placed on the ground in order to prevent mud formation. It was common to use straws for this purpose, so millet could likely have been used in the same way [80].

Another proxy of plant species are *n*-alkanes. In particular, the Average Chain Length (ACL) reveals that they are in part from arboreal origin [66,67]. Another parameter to identify the origin of *n*-alkanes is the comparison between odd and even chains. This parameter reveals that even chains prevail on the odd ones. Normally, plants produce alkanes with a marked predominance of odd chains, so probably these soils were affected by some kind of biological and/or chemical reworking possibly operated by microbes and fire activity, as suggested by De la Rosa et al. (2012) [81]. The predominance of long (C_{24}-C_{35}) over short chains (C_{10}-C_{23}) confirms that the main source of *n*-alkanes is terrestrial vegetation, but the distribution is likely affected by post-depositional effects [68].

7.2 Verona: Via Pigna (VP)

As for the SPM site, the VP samples present a great variability. The two contexts are certainly similar since both sites are located in an urban setting.

Regarding fire events, VP samples show similar results or higher concentration to SPM, in particular high levels of levoglucosan were detected, while in some samples no mannosan and galactosan were present, suggesting prolonged and repeated fires. Probably, also in this case mannosan and galactosan were washed away, also because in these samples levoglucosan shows lower concentrations. The PAHs main compounds are, again, distributed between MMW and HMW. In some samples (VP_A_4, VP_B_3 and VP_B_5) MMW PAHs are more abundant, which could also be

related to a difference in the type and duration of fires in relation to their application (e.g. domestic fireplaces vs productive activities).

Charcoal is more abundant in VP than in SPM, likely meaning that in VP site the accumulation of charred material and ashes was higher, in relation to more intense activities or different destination of the area. An indication of this is also given by the darker color with respect to SPM samples. The higher content of charcoal in VP samples is evidenced also by the presence of larger charcoal particles (< 1000 µm and < 500 µm), that were not detected in the SPM samples. The main contribution to total and organic carbon derives from charcoal also in the VP DE.

Fecal, plant and fungal sterols (FPFS) are present in both sites in a similar concentration range, so we can conclude that the human presence and activity, including livestock breeding, interested the two sites equally and continuously.

The miliacin concentrations are different between the two sampling profiles in Via Pigna (VP_A and VP_B). In particular, concentrations are higher in VP_A (similarly to SPM), while they are lower in VP_B, especially in the deeper samples. This difference could suggest VP_A as an accumulation point for the site, or maybe the use of millet was different: in VP_A it was also employed for building purposes, while in VP_B it was only used as food.

The ACL values are similar between SPM and VP, and the main source are higher plants. The predominance of long chains confirms this hypothesis, while the comparison between odd and even chains underlines again the uncommon predominance of even chains, suggesting a strong reworking of the soils.

7.3 Belluno: Mel (MEL)

The analysis of fire proxies in Mel reveals that PAHs are mainly ascribable to local fires, so the population accumulated the waste from the domestic fireplaces and other activities requiring the use of fire in the neighborhoods. A different information is given by the AMs: there is only levoglucosan, so the origin of biomass burning is cellulose, but the absence of mannosan and galctosan reveal that the waste of fireplace was accumulated, probably, after prolonged exposure to fire. Also, their total absence could be justified as a washing away of these molecules by rainfall and surface runoff. Anyway, the PAHs and AMs give the same information about the use of fire, that fire was employed daily and the domestic fire waste are accumulated in the soil.

Charcoal in MEL samples presented mainly 63 µm particles, like the other two sites, together with bigger charcoal particles, so probably the soil here was less subject to mechanical and biological

reworking. The total and organic carbon is slightly lower than SPM and VP, but also in this case the main responsible for the dark color and the organic carbon content can be identified in charcoal.
The FPFS are lower that at SPM and VP, probably because the population size in Mel was smaller compared to the valley sites. Anyway, the contribution of ruminants is visible in the record, so it is possible to affirm that in MEL site livestock activity was practiced.
The miliacin concentration is very high, so millet probably was used to both feed the animals and people, but also to consolidate the ground.
The ACL index indicates that here alkanes derive mainly from herbaceous plants. The predominance of long chains confirms the hypothesis that *n*-alkanes are from terrestrial plants, while the comparison between odd and even chains underlines a predominance of even chains, likely related to the strong post-depositional reworking that affected these soils.

7.4 Comparison between the sites

The SPM and VP samples presented many similarities, with the exception of the charcoal distribution and abundance, higher at VP. This is because the two sites are adjacent, so it is possible to say that the same or related activities were conducted in the same way in both sites. In particular, the accumulation of waste is present in both sites, so probably it was a common practice. In both sites, fire was employed for domestic and daily use, and then ashes, soot and charcoal were accumulated close to the source. The dark color, characteristic of DE, is slightly different between the two sites, maybe because activities in VP caused slightly higher production and accumulation of charred materials. The miliacin concentration is high in both sites, likely implying that broomcorn millet was consumed and used regularly. The FPFS indices are a direct evidence that the sites were strongly interested by human presence and farming practices. The *n*-alkanes indices propose that the soils were strongly reworked but the origin of *n*-alkanes was essentially from terrestrial plants, in particular from arboreal ones.
In the MEL site the situation is rather different. In particular, the *n*-alkanes origin is from terrestrial plants but mainly from herbaceous ones, so maybe the soil was used also to cultivate some plants in vegetable gardens. The PAHs and AMs inputs suggest that the accumulation was lower than in Verona, also due to the smaller size of the city of Mel. Probably for this reason, also the FPFS contribution is lower, although the activities were similar in the two cities, such as livestock. The charcoal concentration in the MEL site is lower with respect to the Verona sites, similarly to the PAH

and AMs profile. The miliacin concentrations are high also in MEL site, so probably millet was consumed and used intensively there.

Figures 7.1, 7.2, 7.3, 7.4 and 7.5 show the total results from the sampling sites Verona and Mel.

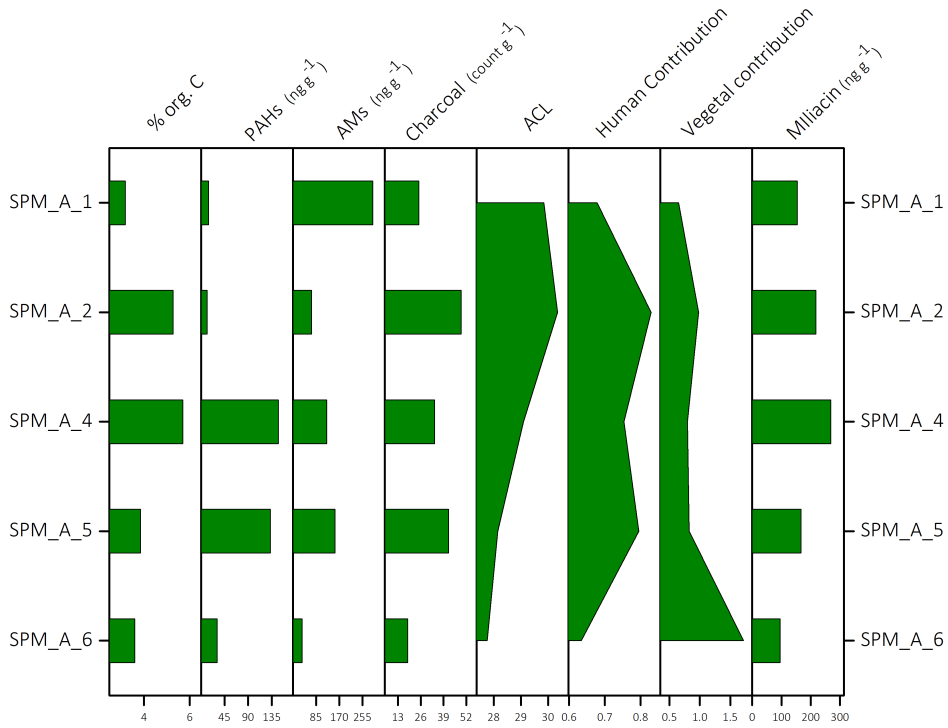

Figure 7.1: Summary of results from SPM_A samples.

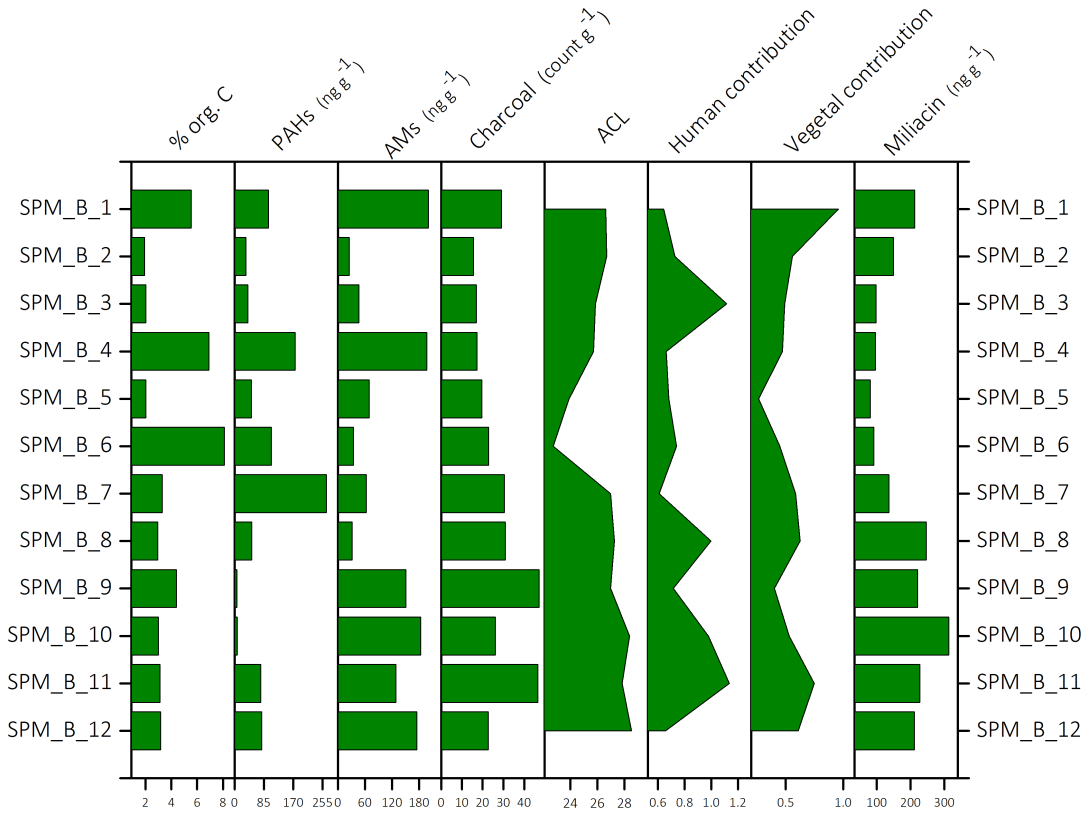

Figure 7.2: Summary of results from SPM_B samples.

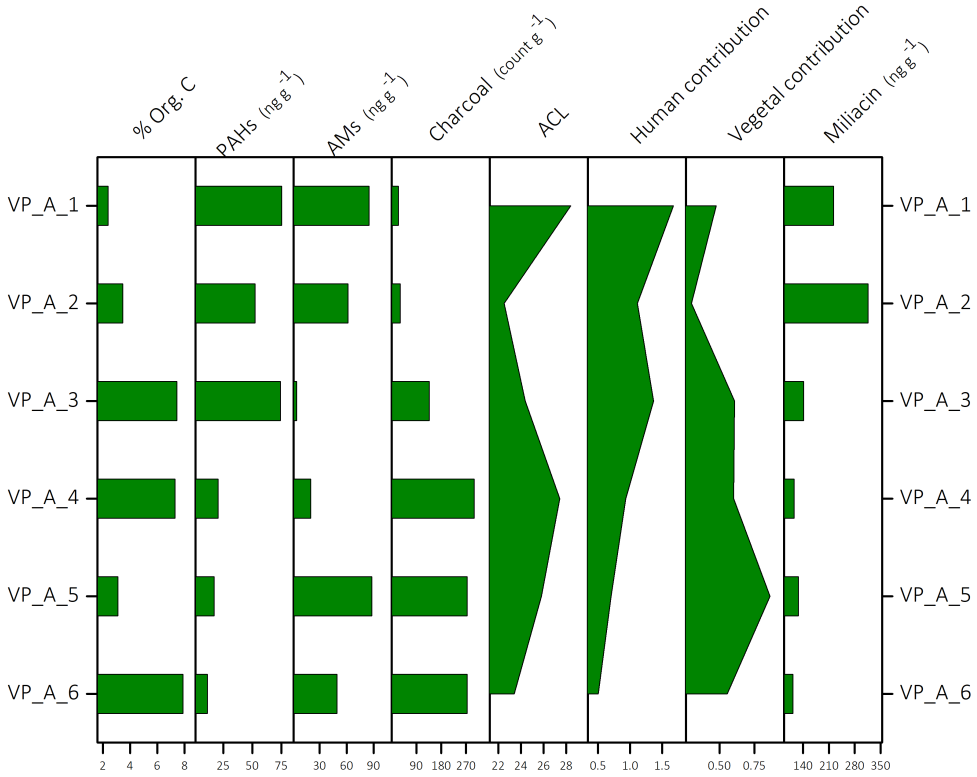

Figure 7.3: Summary of results from VP_A samples.

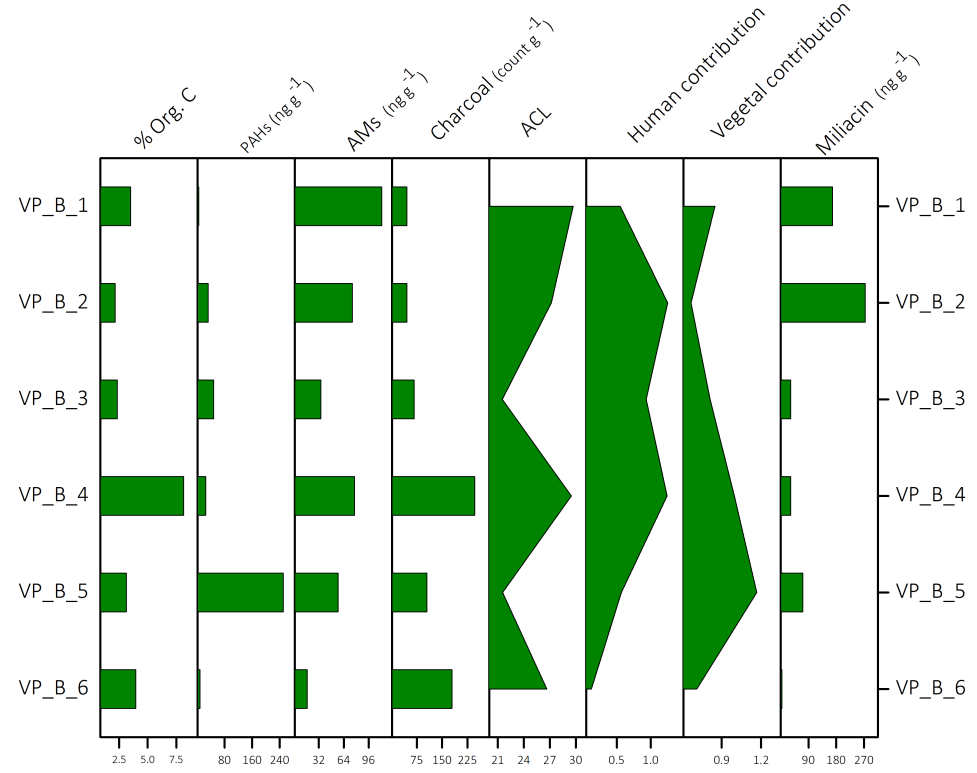

Figure 7.4: Summary of results from VP_B samples.

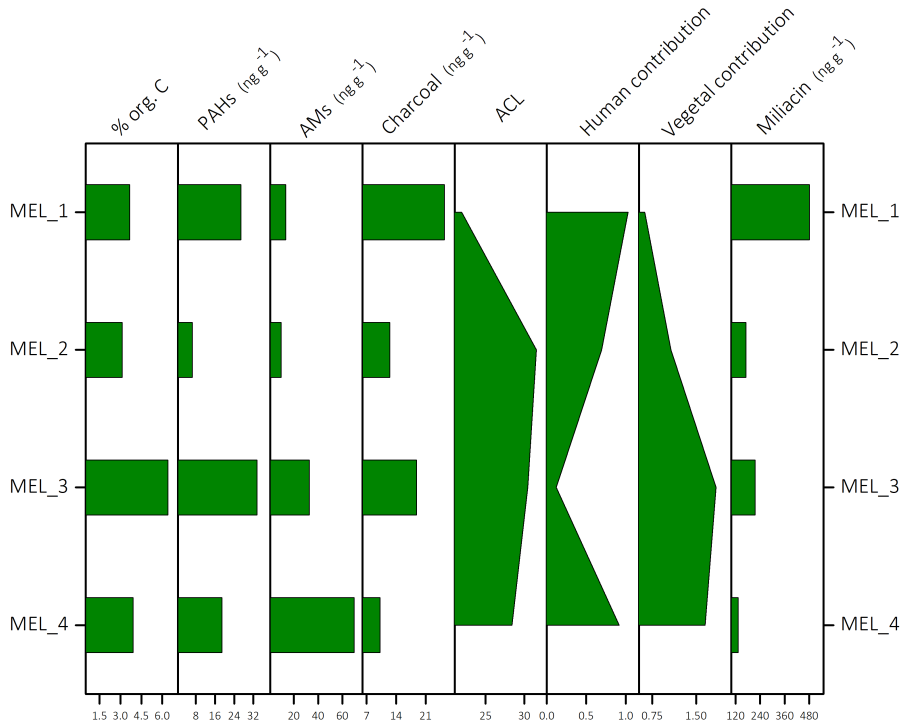

Figure 7.5: Summary of result from MEL samples.

8 CONCLUSIONS

The results from Verona and Mel, combined with literature data, underline that the Dark Earths (DE) soils were strongly reworked and exploited by humans. DE are anthropogenic soils often discovered by chance in urban contexts. These soils are characteristic for their dark color, and the SPM, VP and MEL all have this feature. The dark color is mainly given by the charcoal particles dispersed in the soil. The particles are very numerous, as revealed by the analysis of charcoal distribution. Also, the organic carbon confirms this hypothesis, because the major part of the organic charcoal measured is made of charcoal.

Different hypotheses on the origin of DE were proposed, in particular the most widely accepted are: (i) they result from disposal sites and (ii) they come from agricultural soils, in particular urban cultivation. In the case of SPM, VP and MEL, the Dark Earth is likely originated from waste disposal sites. Some evidence of this hypothesis can be found in the markers that were analyzed. The fire markers, for instance, suggest that the waste from domestic fires were accumulated on the soil. In particular, the high concentrations of MMW and HMW PAHs indicate that the origin of the fire is local. The AMs denote that the charred material was mainly biomass, in particular wood used as a fuel for domestic fires and daily urban activities.

The *n*-alkanes indicate that, probably, vegetation was different between the sites (Verona and Mel), but the main source of is to be identified in plants. However, the soil underwent a strong reworking (continuous mixing, biological and chemical degradation) that affected the distribution of *n*-alkanes. The waste disposal hypothesis is also supported by the investigation of fecal, plant and fungal sterols, whose presence evidences the accumulation of fecal material from humans and ruminants. This interpretation agrees with historical records according to which humans and animals often lived together in unhealthy conditions.

The miliacin concentration indicates that one of the main food sources employed by these people was broomcorn millet. The large concentrations indicate, probably, that millet was not only eaten but also use to feed the animals and the stalks were likely used to consolidate the ground. Also, this large presence of miliacin indicates the accumulation in the waste disposal sites, further supporting the hypothesis formulated from the fire proxies record.

The main difference in the characteristic of DE in Verona and Mel mainly reside in the concentration of analytes. In the Verona sites, the concentrations are slightly higher than in the Mel site, probably because in Verona the inputs were more significant than in Mel. In fact, Mel is a smaller city in the hills, so the condition of living was different with respect to Verona that is in the valley and close to

a big river (Adige), important for trading activities. On the contrary Mel, even nowadays, is a small city. Basically, the activities in these cities were likely similar, such as the practice of farming and minor agricultural practices in vegetable gardens.

Future developments of this project are: the radiocarbon dating, mineralogical and palynological characterization, in order to better know the Dark Earth phenomena.

9 REFERENCES

[1] C. Nicosia, Geoarcheologia delle stratificazioni urbane post-classiche, 2018.

[2] G.P. Brogiolo, M. Cremaschi, S. Gelichi, Processi di stratificazione in centri urbani (dalla stratificazione naturale alla stratificazione archeologica), in: Brescia, 1986: pp. 23–30.

[3] E. Harris, Principles of archaeological stratigraphy, Second edition, Academic Press INC., San Diego, CA 92101, 1997.

[4] Y. Devos, C. Nicosia, L. Vrydaghs, S. Modrie, Studying urban stratigraphy: Dark Earth and a microstratified sequence on the site of the Court of Hoogstraeten (Brussels, Belgium). Integrating archaeopedology and phytolith analysis, Quat. Int. 315 (2013) 147–166. https://doi.org/10.1016/j.quaint.2013.07.024.

[5] Macphil R.I., Galinié H., Verrhaeghe F, A future for dark earth?, 2003.

[6] D. Caporusso, Scavi MM3. Richerche di archeologia urbana a Milano durante la costruzione della line 3 della metropolitana. 1982-1990, (1991).

[7] D. Andrews, D. Perring, Piazza Duomo Lotto Due, 1983.

[8] L. Passi Pitcher, Cremona. Piazza Marconi, in: NotALom, 1983.

[9] S. Gelichi, J. Ortalli, Lo scavo nell'area cortilizia delle Scuole Medie Guinizzelli in via S. Isaia, in: Archeol. Mediev. Bologna Gli Scavi Nel Conv. San Domen., Bologna, 1997: pp. 50–57.

[10] C. La Rocca Hudson, Dark Ages a Verona. Edilizia privata, aree aperte e strutture pubbliche in una città del'Italia settentrionale, in: Archeol. Mediev., 1986: pp. 31–78.

[11] G.P. Brogiolo, S. Gelichi, La città nell'alto medioevo italiano. Archeologia e storia, Bari, 1998.

[12] P. Arthur, Archeologia urbana a Napoli: riflessioni sugli ultimi tre anni, in: Archeol. Mediev., 1986: pp. 515–525.

[13] J. Bruttini, Enclavi urbane a Firenze: il caso della famiglia Uberti, in: Ann. Storia Firenze, 2011: pp. 5–35.

[14] H.D. Foth, Fundamental of soils science, John Weley & sons, 1943.

[15] S. Trevisan, O. Francioso, S. Quaggiotti, S. Nardi, Humic substances biological activity at the plant-soil interface: From environmental aspects to molecular factors, Plant Signal. Behav. 5 (2010) 635–643. https://doi.org/10.4161/psb.5.6.11211.

[16] R.I. Macphail, The Micromorphology of Daerk earth from Gloucaster, London and Norwich: an analysis of urban anthropogenic deposits from Late Roman to Early Medieval periods in England, in: Soil Micromorphol., 1983: pp. 245–252.

[17] Y. Devos, C. Nicosia, L. Vrydaghs, L. Speleers, J. van der Valk, E. Marinova, B. Claes, R.M. Albert,

I. Esteban, T.B. Ball, M. Court-Picon, A. Degraeve, An integrated study of Dark Earth from the alluvial valley of the Senne river (Brussels, Belgium), Quat. Int. 460 (2017) 175–197. https://doi.org/10.1016/j.quaint.2016.06.025.

[18] K. Wiedner, J. Schneeweiß, M.A. Dippold, B. Glaser, Anthropogenic Dark Earth in Northern Germany — The Nordic Analogue to terra preta de Índio in Amazonia, CATENA. 132 (2015) 114–125. https://doi.org/10.1016/j.catena.2014.10.024.

[19] B. Wouters, Y. Devos, K. Milek, L. Vrydaghs, B. Bartholomieux, D. Tys, C. Moolhuizen, N. van Asch, Medieval markets: A soil micromorphological and archaeobotanical study of the urban stratigraphy of Lier (Belgium), Quat. Int. 460 (2017) 48–64. https://doi.org/10.1016/j.quaint.2017.03.002.

[20] R.I. Macphail, The reworking of urban stratigraphy bu human and natural process, in: Symp. Assoc. Environ. Archeol. 12, Oxford, 1994: pp. 13–43.

[21] R.I. Macphail, soil and botanical studies of the “Dark Earth,” in: Environ. Man Iron Age Anglo-Sax. Period, Oxford, 1981: pp. 309–331.

[22] P. Arthur, Naples: a case of urban survival in the early Middle ages, in: Mélanges L’Ecole Fr. Rome Moyen-Age, 1991: pp. 759–784.

[23] P. Arthur, Il particolarismo napoletano altomedievale: una lettura basata sui dati archologici, in: Mélanges L’Ecole Fr. Rome, 1995: pp. 17–30.

[24] M.B. Schiffer, Formation process of the archaeological record, Alburqueque, 1987.

[25] C. Nicosia, R. Langohr, F. Mees, A. Arnoldus-Huyzendveld, J. Bruttini, F. Cantini, Medieval dark earth in an active alluvional setting from Uffizi Gallery complex in Florence, Geoarchaeology. 27 (2012).

[26] C. Nicosia, A. Ertani, A. Vianello, S. Nardi, G.P. Brogiolo, A.C. Arnau, F. Becherini, Heart of darkness: an interdisciplinary investigation of the urban anthropic deposits of the Baptistery of Padua (Italy), Archaeol. Anthropol. Sci. 11 (2019) 1977–1993. https://doi.org/10.1007/s12520-018-0646-2.

[27] R.I. Macphail, M.A. Country, Interpretation and significance of urban deposits, in: Proc. Nord. Conf. Appl. Sci. Methods Archaeol., Helsinki, 1985: pp. 71–83.

[28] B. Yule, The “dark earth” and the late Roman London, 1990.

[29] M. Dotterweich, R. Schreg, Archaeonics - (Geo)archaeological studies in Anthropogenic Dark Earths (ADE) as an example for future-oriented studies of the past, Quat. Int. 502 (2019) 309–318. https://doi.org/10.1016/j.quaint.2018.09.026.

[30] B. Glaser, J.J. Birk, State of the scientific knowledge on properties and genesis of Anthropogenic Dark Earths in Central Amazonia (terra preta de Índio), Geochim. Cosmochim. Acta. 82 (2012) 39–51. https://doi.org/10.1016/j.gca.2010.11.029.

[31] B. Glaser, L. Haumaier, G. Guggenberger, W. Zech, The "Terra Preta" phenomenon: a model for sustainable agriculture in the humid tropics, Naturwissenschaften. 88 (2001) 37–41. https://doi.org/10.1007/s001140000193.

[32] B. Glaser, Prehistorically modified soils of central Amazonian: a model for sustainable agriculture in the twenty-first century, (2007).

[33] C.F.B.V. Alho, A. Samuel-Rosa, G.C. Martins, T. Hiemstra, T.W. Kuyper, W.G. Teixeira, Spatial variation of carbon and nutrients stocks in Amazonian Dark Earth, Geoderma. 337 (2019) 322–332. https://doi.org/10.1016/j.geoderma.2018.09.040.

[34] S. Gasparri, C. La Rocca, Tempi barbarici. L'Europa occidentale tra antichità e medioevo (300-900), Carocci, Città di Castello (PG), 2012.

[35] H. Pirenne, Storia d'Europa dalle inviasioni al XVI secolo, 1917.

[36] U. Büntgen, V. Trouet, D. Frank, H.H. Leuschner, D. Friedrichs, J. Luterbacher, J. Esper, Tree-ring indicators of German summer drought over the last millennium, Quat. Sci. Rev. 29 (2010) 1005–1016. https://doi.org/10.1016/j.quascirev.2010.01.003.

[37] M. Andrič, P. Sabatier, W. Rapuc, N. Ogrinc, M. Dolenec, F. Arnaud, U. von Grafenstein, A. Šmuc, 6600 years of human and climate impacts on lake-catchment and vegetation in the Julian Alps (Lake Bohinj, Slovenia), Quat. Sci. Rev. 227 (2020) 106043. https://doi.org/10.1016/j.quascirev.2019.106043.

[38] U. Buntgen, W. Tegel, K. Nicolussi, M. McCormick, D. Frank, V. Trouet, J.O. Kaplan, F. Herzig, K.-U. Heussner, H. Wanner, J. Luterbacher, J. Esper, 2500 Years of European Climate Variability and Human Susceptibility, Science. 331 (2011) 578–582. https://doi.org/10.1126/science.1197175.

[39] R. Duncan-Jones, Approaching Late Antiquity: The Transformation from Early to Late Empire, Oxford Univ. Press, Oxford, 2004.

[40] M. McCormick, Origins of the European Economy: Communications and Commerce, A.D. 300–900, Camb. Univ Press. (2001).

[41] K.L. Kausrud, M. Begon, T. Ben Ari, H. Viljugrein, J. Esper, U. Buntgen, H. Leirs, C. Junge, B. Yang, M. Yang, L. Xu, N.Chr. Stenseth, Modeling the epidemiological history of plague in Central Asia: Palaeoclimatic forcing on a disease system over the past millennium, BMC Biol.

8 (2010) 112. https://doi.org/10.1186/1741-7007-8-112.

[42] C. Witschel, Re-evaluating the Roman West in the 3rd c. A.D., J. Roman Archaeol. (2004) 251–281. https://doi.org/10.1017/S1047759400008242.

[43] G. Motuzaite-Matuzeviciute, J. Jacob, S. Telizhenko, M.K. Jones, Miliacin in palaeosols from an Early Iron Age in Ukraine reveal in situ cultivation of broomcorn millet, Archaeol. Anthropol. Sci. 8 (2016) 43–50. https://doi.org/10.1007/s12520-013-0142-7.

[44] N. Bossard, J. Jacob, C. Le Milbeau, J. Sauze, V. Terwilliger, B. Poissonnier, E. Vergès, Distribution of miliacin (olean-18-en-3β-ol methyl ether) and related compounds in broomcorn millet (Panicum miliaceum) and other reputed sources: Implications for the use of sedimentary miliacin as a tracer of millet, Org. Geochem. 63 (2013) 48–55. https://doi.org/10.1016/j.orggeochem.2013.07.012.

[45] N. Dubois, J. Jacob, Molecular Biomarkers of Anthropic Impacts in Natural Archives: A Review, Front. Ecol. Evol. 4 (2016). https://doi.org/10.3389/fevo.2016.00092.

[46] K.H. Freeman, R.D. Pancost, Biomarkers for Terrestrial Plants and Climate, in: Treatise Geochem., Elsevier, 2014: pp. 395–416. https://doi.org/10.1016/B978-0-08-095975-7.01028-7.

[47] C. Nicosia, Geoarcheologia delle stratificazioni urbane post-classiche, 2018.

[48] C. Whitlock, C. Larsen, Charcoal as a Fire Proxy, in: J.P. Smol, H.J.B. Birks, W.M. Last, R.S. Bradley, K. Alverson (Eds.), Track. Environ. Change Using Lake Sediments, Springer Netherlands, Dordrecht, 2002: pp. 75–97. https://doi.org/10.1007/0-306-47668-1_5.

[49] E. Eckmeier, R. Gerlach, J.O. Skjemstad, M.W.I. Schmidt, Only small changes in soil organic carbon and charcoal found one year after experimental slash-and-burn in a temperate deciduous forest., Biogeosciences. (2007).

[50] E. Eckmeier, M. Rösch, O. Ehrmann, M.W.I. Schmidt, W. Schier, R. Gerlach, Conversion of biomass to charcoal and the carbon mass balance from a slash-and- burn experiment in a temperate deciduous forest., Holocene. (2007).

[51] A.C. Scott, Preservation by fire, in: Briggs DEG Crowther PJ Eds, Blackwells, Oxford, 2001: pp. 277–280.

[52] G.J. Nichols, J. Cripps, M.E. Collinson, A.C. Scott, Experiments in waterlogging and sedimentology of charcoal: results and implications., Palaeogeogr. Palaeoclimatol. Palaeoecol. (2000).

[53] M.S. Forbes, R.J. Raison, J.O. Skjemstad, Formation, transformation and transport of black

carbon (charcoal) in terrestrial and aquatic ecosystems., Sci. Total Environ. (2006).

[54] A.C. Scott, The Pre-Quaternary history of fire, Palaeogeogr. Palaeoclimatol. Palaeoecol. (2000).

[55] S.J. Pyne, P.L. Andrews, R.D. Laven, Introduction to Wildland Fire, Wiley and Sons, New York, 1996.

[56] A.C. Scott, Charcoal recognition, taphonomy and uses in palaeoenvironmental analysis, Palaeogeogr. Palaeoclimatol. Palaeoecol. 291 (2010) 11–39. https://doi.org/10.1016/j.palaeo.2009.12.012.

[57] B.R.T. Simoneit, Biomass burning — a review of organic tracers for smoke from incomplete combustion, Appl. Geochem. 17 (2002) 129–162. https://doi.org/10.1016/S0883-2927(01)00061-0.

[58] E.H. Denis, J.L. Toney, R. Tarozo, R. Scott Anderson, L.D. Roach, Y. Huang, Polycyclic aromatic hydrocarbons (PAHs) in lake sediments record historic fire events: Validation using HPLC-fluorescence detection, Org. Geochem. 45 (2012) 7–17. https://doi.org/10.1016/j.orggeochem.2012.01.005.

[59] E. Argiriadis, D. Battistel, D.B. McWethy, M. Vecchiato, T. Kirchgeorg, N.M. Kehrwald, C. Whitlock, J.M. Wilmshurst, C. Barbante, Lake sediment fecal and biomass burning biomarkers provide direct evidence for prehistoric human-lit fires in New Zealand, Sci. Rep. 8 (2018) 12113. https://doi.org/10.1038/s41598-018-30606-3.

[60] M.O. Andreae, P. Merlet, Emission of trace gases and aerosols from biomass burning., Glob. Biogeochem. Cycles. (2008). https://doi.org/10.1029/2000GB001382.

[61] E.M. Rubin, Genomics of cellulosic biofuels., Nature. (2008). https://doi.org/10.1038/nature07190.

[62] V.O. Elias, B.R.T. Simoneit, R.C. Cordeiro, B. Turcq, Evaluating levoglucosan as an indicator of biomass burning in Carajàs, Amazonia: A comparison to the charcoal record, (2001).

[63] B.R.T. Simoneit, J.J. Schauer, G.C. Nolte, D.R. Oros, V.O. Elias, M.P. Fraser, W.F. Rogge, G.R. Cass, Levoglucosan, a tracer for cellulose in biomass burning and atmospheric particles., Atmos. Environ. (n.d.). https://doi.org/10.1016/S1352-2310(98)00145-9.

[64] L.-J. Kuo, P. Louchouarn, B.E. Herbert, Influence of combustion conditions on yields of solvent-extractable anhydrosugars and lignin phenols in chars: Implications for characterizations of biomass combustion residues., Chemosphere. (2011). https://doi.org/10.1016/j.chemosphere.2011.06.074.

[65] K. Janoszka, M. Czaplicka, Methods for the determination of levoglucosan and other sugar anhydrides as biomass burning tracers in environmental samples - A review, J. Sep. Sci. 42 (2019) 319–329. https://doi.org/10.1002/jssc.201800650.

[66] A. Callegaro, D. Battistel, N.M. Kehrwald, F. Matsubara Pereira, T. Kirchgeorg, M. del C. Villoslada Hidalgo, B.W. Bird, C. Barbante, Fire, vegetation, and Holocene climate in a southeastern Tibetan lake: a multi-biomarker reconstruction from Paru Co, Clim. Past. 14 (2018) 1543–1563. https://doi.org/10.5194/cp-14-1543-2018.

[67] A. El Nemr, A.A. Moneer, S. Ragab, A. El Sikaily, Distribution and sources of n-alkanes and polycyclic aromatic hydrocarbons in shellfish of the Egyptian Red Sea coast, Egypt. J. Aquat. Res. 42 (2016) 121–131. https://doi.org/10.1016/j.ejar.2016.05.003.

[68] P.A. Cranwell, G. Eglinton, N. Robinson, Lipids of aquatic organisms as potential contributors to lacustrine sediments--II, (n.d.) 15.

[69] M. Wang, W. Zhang, J. Hou, Is average chain length of plant lipids a potential proxy for vegetation, environment and climate changes?, Biogeosciences Discuss. 12 (2015) 5477–5501. https://doi.org/10.5194/bgd-12-5477-2015.

[70] J. Jacob, J.-R. Disnar, G. Bardoux, Carbon isotope evidence for sedimentary miliacin as a tracer of Panicum miliaceum (broomcorn millet) in the sediments of Lake le Bourget (French Alps), Org. Geochem. 39 (2008) 1077–1080. https://doi.org/10.1016/j.orggeochem.2008.04.003.

[71] G. Ganzarolli, M. Alexander, A. Chavarria Arnau, O.E. Craig, Direct evidence from lipid residue analysis for the routine consumption of millet in Early Medieval Italy, J. Archaeol. Sci. 96 (2018) 124–130. https://doi.org/10.1016/j.jas.2018.06.007.

[72] R. Zocatelli, M. Lavrieux, T. Guillemot, L. Chassiot, C. Le Milbeau, J. Jacob, Fecal biomarker imprints as indicators of past human land uses: Source distinction and preservation potential in archaeological and natural archives, J. Archaeol. Sci. 81 (2017) 79–89. https://doi.org/10.1016/j.jas.2017.03.010.

[73] J.J. Birk, W.G. Teixeira, E.G. Neves, B. Glaser, Faeces deposition on Amazonian Anthrosols as assessed from 5β-stanols, J. Archaeol. Sci. 38 (2011) 1209–1220. https://doi.org/10.1016/j.jas.2010.12.015.

[74] D. Battistel, R. Piazza, E. Argiriadis, E. Marchiori, M. Radaelli, C. Barbante, GC-MS method for determining faecal sterols as biomarkers of human and pastoral animal presence in freshwater sediments, Anal. Bioanal. Chem. 407 (2015) 8505–8514. https://doi.org/10.1007/s00216-015-8998-2.

[75] I.D. Bull, M.J. Lockheart, M.M. Elhmmali, D.J. Roberts, R.P. Evershed, The origin of faeces by means of biomarker detection, Environ. Int. 27 (2002) 647–654. https://doi.org/10.1016/S0160-4120(01)00124-6.

[76] J.D. Weete, M. Abril, M. Blackwell, Phylogenetic Distribution of Fungal Sterols, PLoS ONE. 5 (2010) e10899. https://doi.org/10.1371/journal.pone.0010899.

[77] I.S. Castañeda, S. Schouten, A review of molecular organic proxies for examining modern and ancient lacustrine environments, Quat. Sci. Rev. 30 (2011) 2851–2891. https://doi.org/10.1016/j.quascirev.2011.07.009.

[78] M. Derrien, L. Yang, J. Hur, Lipid biomarkers and spectroscopic indices for identifying organic matter sources in aquatic environments: A review, Water Res. 112 (2017) 58–71. https://doi.org/10.1016/j.watres.2017.01.023.

[79] D. Battistel, E. Argiriadis, N. Kehrwald, M. Spigariol, J.M. Russell, C. Barbante, Fire and human record at Lake Victoria, East Africa, during the Early Iron Age: Did humans or climate cause massive ecosystem changes?, The Holocene. 27 (2017) 997–1007. https://doi.org/10.1177/0959683616678466.

[80] A. Bruttomesso, V. Frisone, R. Ghiotto, Il museo civico Giuseppe Zannato di Montecchio Maggiore, Canova, 2014.

[81] J.M. De la Rosa, S.R. Faria, M.E. Varela, H. Knicker, F.J. González-Vila, J.A. González-Pérez, J. Keizer, Characterization of wildfire effects on soil organic matter using analytical pyrolysis, Geoderma. 191 (2012) 24–30. https://doi.org/10.1016/j.geoderma.2012.01.032.